Advances in Nano Research, *Vol. 11, No. 5 (2021) 547-563*
https://doi.org/10.12989/anr.2021.11.5.547

On the modeling and simulation of the nonlinear dynamic response of NEMS via a couple of nonlocal strain gradient theory and classical beam theory

Jian Zhao[1] and Zhuo Yu*[2]

[1]*School of Information Science and Technology, Northwest University, Xian 710127, Shaanxi, China*
[2]*School of Computer Science and Engineering, North Minzu University, Yinchuan 750021, Ningxia, China*

(*Received August 8, 2021, Revised October 16, 2021, Accepted October 17, 2021*)

Abstract. In the present research, the dynamic characteristics of the nanoscale tubes and pipes with nonuniform cross-sections are examined. The aforementioned nanostructures are made by imperfect axially functionally graded materials (AFGM) that compose ceramic and metal phases along the tube length direction, involving the porous voids. To this purpose, the Hamilton principle is implemented to obtaining the governing equation and related boundary conditions using classical beam theory coupled to the nonlinear Von-Kármán theory. In order to apply the size impact, the nonlocal strain gradient theory is considered that both hardening and softening parameters are involved. Also, iteration techniques, including the generalized differential quadrature method (GDQM), are used to solve linear and nonlinear derived partial differential equations (PDE). Finally, the obtained results are explained in detail to investigate the impact of nonlinear amplitude, nonlocal and strain gradient parameter, porosity parameter, etc., for both clamped and simply-supported types of boundary conditions, which are helpful to design the nanoelectromechanical structures (NEMS).
Keywords: axially functionally graded tube; gradient strain theory; imperfect; nonlinear vibration; non-uniform; porous; tapered tube; truncated conical tube

1. Introduction

Nanostructures have played an important role in the advancement of sciences, engineering, and new nanotechnologies. Nanomaterials are gaining popularity owing to their unique features that influence biological, chemical, optoelectrical, electrical, and physical properties. The focus on nanostructures is one of the most important subjects that attracts many academics to develop these studies concerning the behavior of nanostructures. Many scientists have focused their efforts in recent years on creating nanoscience in many areas, particularly nanomechanics, such as nano-scale beams, microbeams, nanoplates, and many other structures in nano and micro sizes (Hamidi *et al*. 2015, Allahkarami *et al*. 2017, Ehyaei *et al*. 2017, Akbas 2018a, b, Arefi and Zenkour 2018, Aydogdu *et al*. 2018, Bensaid *et al*. 2018, Navi *et al*. 2019, Ebrahimi *et al*. 2020, Gafour *et al*. 2020, Matouk *et al*. 2020, Ni *et al*. 2020, Zhao *et al*. 2020, 2021, Guo *et al*. 2021, Hu *et al*. 2021, Li *et al*. 2021, Liu *et al*. 2021a, b, c, Lu *et al*. 2021, Ni *et al*. 2021, Wang *et al*. 2021, Zhang *et al*. 2021a, b, Zhong *et al*. 2021).

Vibration of nano beams and tubes are of great importance in the past years in the literature. Besseghier *et al*. (2015) studied the nonlinear vibration of a zigzag shaped nanotube using Winkler-type model to consider the interaction of the zigzag nanotube with the surrounding elastic medium. Alibeigloo and Emtehani (2015) used the three dimensional theory of elasticity to study the vibration of carbon nanotubes reinforced composite (CNTRC) plates. Mirzaei and Kiani (2016) investigated the large amplitude free vibrations of a sandwich beam with stiff core and carbon nanotube (CNT)-reinforced face sheets. Wang *et al*. (2016) introduced the multi-term Kantorovich–Galerkin method to analyze the buckling and vibration of thin carbon nanotube-reinforced composite (CNTRC) plates with the classical plate theory. Lu *et al*. (2017) studied the size-dependent sinusoidal shear deformation nanobeam model to investigate the free vibration of nanobeams based on the nonlocal strain gradient theory. Ghadiri and Shafiei (2016) studied the small scale effect on the nonlinear bending vibration of a rotating cantilever and propped cantilever nanobeam. Investigation on free vibration of nanobeams based on Eringen nonlocal elasticity theory and Timoshenko beam theory is presented by Ebrahimi and Nasirzadeh (2015).

Functionally graded materials (FGM) have been used and studied for many applications such as sensors (Mueller *et al*. 2003), biomedical applications (Pompe *et al*. 2003), thermal barrier coatings (Lee *et al*. 1996), orthopedic applications (Bekkaye *et al*. 2020, Zine *et al*. 2020, Arshid *et al*. 2021, Bellifa *et al*. 2021, Guellil *et al*. 2021, Hadji *et al*. 2021, Kumar *et al*. 2021, Tahir *et al*. 2021a, b), automotive applications (Srinivas *et al*. 2019), biological materials (Liu *et al*. 2017) and etc (Bai *et al*. 2020, Li *et al*. 2020a, b, Al-Furjan *et al*. 2021a, b, c, d, Dai *et al*. 2021a, b, Guo *et al*. 2021, Habibi *et al*. 2021, Huo *et al*. 2021, Shi *et al*. 2020, Wang *et al*. 2020, Zhou *et al*. 2020, Najaafi *et al*. 2021, Peng *et al*. 2021, Shao *et al*. 2021, Wu and Habibi

*Corresponding author, MS.,
E-mail: 20207152@stu.nun.edu.cn

ISSN: 2287-237X (Print), 2287-2388 (Online)

2021, Zhang *et al*. 2021). These various applications made the researchers to study the vibrational behavior of nanosystems which are made by FGMs. Zhang *et al*. (2015) studied the frequencies of functionally graded carbon nanotube-reinforced composite (FG-CNTRC) skew plates and the mode shapes of them with the transverse shear deformation. Şimşek (2016) used nonlocal size-dependent nonlinear vibration of functionally graded nanobeam. The thermo-mechanical vibration behavior of two dimensional functionally graded (2D-FG) porous nanobeam is studied by Mirjavadi *et al*. (2017). Shafiei *et al*. (2016) studied nonlinear vibration of rotating Euler–Bernoulli porous nanobeam considering the small-scale effect. Mirjavadi *et al*. (2017) considered the thermal effect in their investigation on the buckling and free vibration of axially functionally graded nanobeam. Mohammadi *et al*. (2019) considered mechanical an electrical loads on nonlinear vibration porous functionally graded Euler-Bernoulli nanobeam. In another study, Tong *et al*. (2020) studied the stability of functionally graded nanotube with cantilever boundary condition, also, wave propagation in embedded functionally graded nanotubes conveying fluid is studied (Filiz and Aydogdu 2015).

It is apparent from the numerous experiments given that various parameter effects affect the nonlinear response of FG tubes. Despite the availability of many references on nonlinear responses of nanostructures, no reference has been given to explore the nonlinear behavior of an AFG tapered and imperfect nanotube with nonlinear nonlocal boundary conditions. As a result, more research into the nonlinear vibrational of functionally graded truncated conical nanosized tubes with porosity is required. For the first time, this article examines the nonlinear analysis of a nonuniform porosity-dependent nanotube constructed of metal and ceramic graded material, taking into account von-nonlinear Kármán's strain. The nonlinear equations and nonlinear nonlocal boundary conditions are obtained using the Hamilton principle, and they are solved using GDQ and the iteration technique for the classical Euler-Bernoulli beam theory.

2. Conceptualization and formulation

2.1 Tubes structures

Along Fig. 1, in the axial direction of the tube, a combination of a metal (at x=0) and a ceramic (at x=L) phase produces a tapered AFG-nanotube with lengths 'L', 'Ri', and 'Ro', as well as inner and outer radiuses. The material variation leads to a variation in all the nanotube's mechanical properties following the relation in Eq. (1), where "n_R" indicates the FG power index (Shafiei and Kazemi 2017).

$$F(r) = F_m + (F_c - F_m)\left(\frac{x}{L}\right)^n \tag{1}$$

The $()_c$ and $()_m$ indices represent ceramic and metal, respectively, and '*r*' is the distance from the center of the FG tube. The linear function of radius changes the radius of

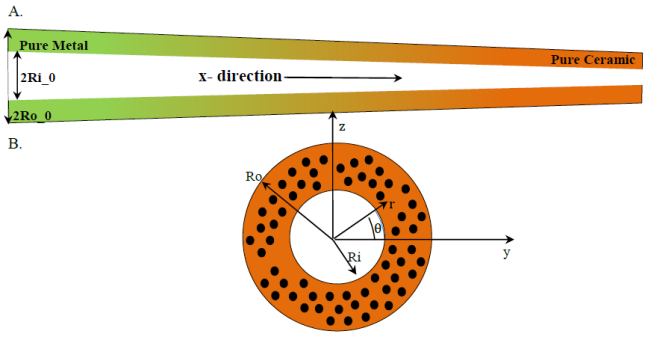

Fig. 1 The non-uniform cross-section and material change of the Functionally graded porous nano-tube throughout its length

Table 1 The mechanical characteristics of several ceramic and metal phases, involving Young's modulus, Poison ratio, and mass density (Reddy and Chin 1998)

Properties	SUS304	Si_3N_4
E (Pa)	2.0779e+11	3.22269e+11
ν	0.3177	0.24
ρ (Kg/m^3)	8166	2370

the non-uniform cross-section tube throughout its length; the linear function of radius is:

$$r = R_0\left(1+\beta_R\left(\frac{x}{L}\right)\right) \tag{2}$$

R_0 indicates the radius in the left side (at x = 0) of the tube, and β_R is the rate of cross-section changes. Both inner and outer radius are applied by this function. The equations for Young's modulus (E), Poisson's ratio (ν), and mass density (ρ) equations of the FG nanotube can be expressed as:

$$E(x) = \left[E_m + (E_c - E_m)\left(\frac{x}{L}\right)^n\right]\left(1-\alpha\cos\left(\pi\frac{r-R_i}{R_0-R_i}\right)\right) \tag{3a}$$

$$\nu(x) = \left[\nu_m + (\nu_c - \nu_m)\left(\frac{x}{L}\right)^n\right]\left(1-\alpha\cos\left(\pi\frac{r-R_i}{R_0-R_i}\right)\right) \tag{3b}$$

$$\rho(x) = \left[\rho_m + (\rho_c - \rho_m)\left(\frac{x}{L}\right)^n\right]\left(1-\alpha\cos\left(\pi\frac{r-R_i}{R_0-R_i}\right)\right) \tag{3c}$$

α ($0 \le \alpha \ll 1$) is the volume fraction of porosity (Shafiei and Kazemi 2017). The mechanical properties of different ceramics and metals are shown in Table 1. The coordinate system is considered as cylindrical O (x, r, θ). In this coordinate system, x, r and θ define the length, radial, and circumferential directions, respectively. The coordinate system to refer the nanotube is rectangular O (x, y, z), where u_1, u_2, and u_3 denote the appropriate displacement components are as follows:

$$y, z = r(\cos(\theta), \sin(\theta)); \qquad y^2 + z^2 = r^2 \tag{4}$$

2.2 Mathematical modeling

The classical beam model is used to calculate the displacement of the nanotube's point, as shown below:

$$\begin{aligned} u_1(x,z,t) &= z\,\varphi + u(x,t) \\ u_2 &= 0 \\ u_3(x,t) &= w(x,t) \end{aligned} \tag{5}$$

The transverse displacement and rotation angle around the *y* axis are represented by *w*(*x*) and '$\varphi = -\partial w/\partial x$', respectively. Also, where u_1 , u_2 and u_3 are the displacement field components along the *x*, *y*, and *z* axes. The nonlinear strains are defined as follows using the nonlinear Von-Kármán theory linked with the classical and first-order shear deformation beam theory:

$$\varepsilon_{xx} = \frac{\partial u_1}{\partial x} = \frac{\partial u}{\partial x} - z\,\frac{\partial^2 w}{\partial x^2} + \frac{1}{2}\left(\frac{\partial w}{\partial x}\right)^2 \tag{6a}$$

$$\varepsilon_{xy} = \varepsilon_{xz} = 0 \tag{6b}$$

stresses are defined as:

$$\sigma_{xx} = E\,\varepsilon_{xx} \tag{7a}$$

$$\sigma_{xy} = \sigma_{xz} = 0 \tag{7b}$$

The Hamiltonian principle is used to derive the governing equations as well as the boundary conditions equations (Hou *et al*. 2021, Huang *et al*. 2021a, b, c, Jiao *et al*. 2021, Liu *et al*. 2021 a, b, c, Ma *et al*. 2021, Moradi *et al*. 2021, Xu *et al*. 2021, Zhao *et al*. 2021, Yu *et al*. 2022). It is explained as follows:

$$\int_{t_1}^{t_2} \delta H dt = \int_{t_1}^{t_2} (\delta K - \delta S + \delta V)\,dt = 0 \tag{8}$$

where *K*, *S*, and *V* denote, respectively, kinetic energy, strain energy, and external work. Transversally, the displacement is believed to be considerable, whereas the rotation is believed to be minor. The following equation is used to determine the nanotube's virtual strain energy:

$$\delta S = \iiint \delta s dv = \int_0^L \left[\begin{array}{l} A_{11}\frac{\partial u}{\partial x}\delta\left(\frac{\partial u}{\partial x}\right) + D_{11}\frac{\partial^2 w}{\partial x^2}\delta\left(\frac{\partial^2 w}{\partial x^2}\right) + \frac{1}{2}\left(\frac{\partial w}{\partial x}\right)^2 \delta\left(\frac{\partial u}{\partial x}\right) \\ + A_{11}\left(\frac{1}{2}\left(\frac{\partial w}{\partial x}\right)^3 \delta\left(\frac{\partial w}{\partial x}\right) + \frac{\partial u}{\partial x}\frac{\partial w}{\partial x}\delta\left(\frac{\partial w}{\partial x}\right)\right) \end{array}\right] dx \tag{9}$$

where

$$(A_{11}(x), D_{11}(x)) = \iint_A E(x,r)(1, z^2)\,dA \tag{10}$$

The kinetic energy is derived as:

$$\begin{aligned} \delta K &= \delta \iiint k dv = \frac{1}{2}\delta \int_0^L \iint_A \rho(x,r)\left(\left(\frac{\partial u_x}{\partial t}\right)^2 + \left(\frac{\partial u_y}{\partial t}\right)^2 + \left(\frac{\partial u_z}{\partial t}\right)^2\right) dA\,dx \\ &= \int_0^L \left\{ m_0\left[\frac{\partial u}{\partial t}\delta\left(\frac{\partial u}{\partial t}\right) + \frac{\partial w}{\partial t}\delta\left(\frac{\partial w}{\partial t}\right)\right] + m_2\frac{\partial^2 w}{\partial x\,\partial t}\delta\left(\frac{\partial^2 w}{\partial x\,\partial t}\right)\right\} dx \end{aligned} \tag{11}$$

where

$$(m_0(x), m_2(x)) = \iint_A \rho(x,r)(1, z^2)\,dA \tag{12}$$

External work (V) has been set to zero.

$$\delta V = 0 \tag{13}$$

The following Euler–Lagrange equation has been found by substituting Eqs. ((9), (11) and (13) into Eq. (8) and assuming that δu, δw and δψ are all zero:

$$\delta u : -\frac{\partial}{\partial x}\left(A_{11}\frac{\partial u}{\partial x} + \frac{1}{2}A_{11}\left(\frac{\partial w}{\partial x}\right)^2\right) = m_0\frac{\partial^2 u}{\partial t^2} \tag{14a}$$

$$\delta w : \frac{\partial^2}{\partial x^2}\left(D_{11}\frac{\partial^2 w}{\partial x^2}\right) + \frac{\partial}{\partial x}\left[\left(A_{11}\frac{\partial u}{\partial x} + \frac{1}{2}A_{11}\left(\frac{\partial w}{\partial x}\right)^2\right)\frac{\partial w}{\partial x}\right] = m_0\frac{\partial^2 w}{\partial t^2} - m_2\frac{\partial^4 w}{\partial x^2\partial t^2} \tag{14b}$$

Furthermore, the following are the boundary conditions:

$$u = 0 \quad \text{or} \quad N = 0 \tag{15a}$$

$$\partial w/\partial x = 0 \quad \text{or} \quad M = 0 \tag{15b}$$

$$w = 0 \quad \text{or} \quad \partial M/\partial x = 0 \tag{15c}$$

where

$$N = A_{11}\frac{\partial u}{\partial x} + \frac{1}{2}A_{11}\left(\frac{\partial w}{\partial x}\right)^2 \tag{16a}$$

$$M = D_{11}\frac{\partial^2 w}{\partial x^2} \tag{16b}$$

2.3 Nonlocal strain gradient theory

Lim *et al*. (2015) developed nonlocal strain gradient theory by combining Eringen (1983) nonlocal stress theory with Aifantis (1992) and Mindlin (1965) strain gradient theory. The total stress tensor t_{xx} is calculated using the nonlocal strain gradient theory as follows:

$$\left[1 - (ea)^2\nabla^2\right] t_{xx} = E\left(1 - l^2\nabla^2\right)\varepsilon_{xx} \tag{17}$$

where "*ea*" and "*l*" are nonlocal and strain gradient parameters. The stress resultants in Eq. (16) revised as below utilizing the nonlocal strain gradient theory:

$$N = \left(1 - l^2\frac{\partial^2}{\partial x^2}\right)(N) + (ea)^2\frac{\partial}{\partial x}\left(m_0\frac{\partial^2 u}{\partial t^2}\right) \tag{18a}$$

$$M = M - l^2\frac{\partial^2 M}{\partial x^2} + (ea)^2\left(m_0\frac{\partial^2 w}{\partial t^2} - m_2\frac{\partial^4 w}{\partial x^2\partial t^2} - \frac{\partial}{\partial x}\left((N)\frac{\partial w}{\partial x}\right)\right) \tag{18b}$$

As a consequence of the nonlocal strain gradient theory, the vibration equation for the FG nanotube is as follows.
δu:

$$\frac{\partial}{\partial x}\left(\left(l^2\frac{\partial^2}{\partial x^2} - 1\right)\left(+\frac{1}{2}A_{11}\left(\frac{\partial w}{\partial x}\right)^2 + A_{11}\frac{\partial u}{\partial x}\right)\right) = -(ea)^2\frac{\partial^2}{\partial x^2}\left(m_0\frac{\partial^2 u}{\partial t^2}\right) + m_0\frac{\partial^2 u}{\partial t^2} \tag{19a}$$

$$\begin{aligned}\delta w :&\frac{\partial^2}{\partial x^2}\left(D_{11}\frac{\partial^2 w}{\partial x^2}-l^2\frac{\partial^2}{\partial x^2}\left(D_{11}\frac{\partial^2 w}{\partial x^2}\right)\right)-\frac{\partial}{\partial x}\left(\begin{array}{l}\left(\begin{array}{l}A_{11}\dfrac{\partial u}{\partial x}+\dfrac{1}{2}A_{11}\left(\dfrac{\partial w}{\partial x}\right)^2\\ \qquad\dfrac{\partial^2\left(A_{11}\dfrac{\partial u}{\partial x}+\dfrac{1}{2}A_{11}\left(\dfrac{\partial w}{\partial x}\right)^2\right)}{\partial x^2}\\ -l^2\end{array}\right)\dfrac{\partial w}{\partial x}\end{array}\right)\\ &+(ea)^2\frac{\partial^2}{\partial x^2}\left(\frac{\partial}{\partial x}\left(\left(\left(A_{11}\frac{\partial u}{\partial x}+\frac{1}{2}A_{11}\left(\frac{\partial w}{\partial x}\right)^2-l^2\frac{\partial^2}{\partial x^2}\left(A_{11}\frac{\partial u}{\partial x}+\frac{1}{2}A_{11}\left(\frac{\partial w}{\partial x}\right)^2\right)\right)\right)\frac{\partial w}{\partial x}\right)\right)\\ &=+m_0\frac{\partial^2 w}{\partial t^2}-m_1\frac{\partial^4 w}{\partial x^2\partial t^2}-(ea)^2\frac{\partial^2}{\partial x^2}\left(m_0\frac{\partial^2 w}{\partial t^2}-m_1\frac{\partial^4 w}{\partial x^2\partial t^2}\right)\end{aligned} \tag{19b}$$

The nonlocal nonlinear boundary conditions are

$$u = 0 \text{ or } \begin{array}{l}A_{11}\dfrac{\partial u}{\partial x}+\dfrac{1}{2}A_{11}\left(\dfrac{\partial w}{\partial x}\right)^2-l^2\dfrac{\partial^2}{\partial x^2}\left(A_{11}\dfrac{\partial u}{\partial x}+\dfrac{1}{2}A_{11}\left(\dfrac{\partial w}{\partial x}\right)^2\right)\\ +(ea)^2\dfrac{\partial}{\partial x}\left(m_0\dfrac{\partial^2 u}{\partial t^2}\right)=0\end{array} \tag{20a}$$

$$w = 0 \text{ or } \begin{array}{l}\dfrac{\partial}{\partial x}\left(D_{11}\dfrac{\partial^2 w}{\partial x^2}\right)-l^2\dfrac{\partial^3}{\partial x^3}\left(D_{11}\dfrac{\partial^2 w}{\partial x^2}\right)\\ +(ea)^2\dfrac{\partial}{\partial x}\left(\begin{array}{l}m_0\dfrac{\partial^2 w}{\partial t^2}-m_2\dfrac{\partial^4 w}{\partial x^2\partial t^2}\\ -\dfrac{\partial}{\partial x}\left[\left(\begin{array}{l}A_{11}\dfrac{\partial u}{\partial x}+\dfrac{1}{2}A_{11}\left(\dfrac{\partial w}{\partial x}\right)^2\\ -l^2\dfrac{\partial^2}{\partial x^2}\left(A_{11}\dfrac{\partial u}{\partial x}+\dfrac{1}{2}A_{11}\left(\dfrac{\partial w}{\partial x}\right)^2\right)\end{array}\right)\dfrac{\partial w}{\partial x}\right]\end{array}\right)=0\end{array} \tag{20b}$$

$$\partial w/\partial x = 0 \text{ } \begin{array}{l}M = D_{11}\dfrac{\partial^2 w}{\partial x^2}-l^2\dfrac{\partial^2}{\partial x^2}\left(D_{11}\dfrac{\partial^2 w}{\partial x^2}\right)\\ +(ea)^2\left(\begin{array}{l}m_0\dfrac{\partial^2 w}{\partial t^2}-m_2\dfrac{\partial^4 w}{\partial x^2\partial t^2}\\ -\dfrac{\partial}{\partial x}\left[\left(\begin{array}{l}A_{11}\dfrac{\partial u}{\partial x}+\dfrac{1}{2}A_{11}\left(\dfrac{\partial w}{\partial x}\right)^2\\ -l^2\dfrac{\partial^2}{\partial x^2}\left(A_{11}\dfrac{\partial u}{\partial x}+\dfrac{1}{2}A_{11}\left(\dfrac{\partial w}{\partial x}\right)^2\right)\end{array}\right)\dfrac{\partial w}{\partial x}\right]\end{array}\right)=0\end{array} \tag{20c}$$

The expanded equations are:

$$\begin{aligned}\delta w :&\frac{\partial^2}{\partial x^2}\left(D_{11}\frac{\partial^2 w}{\partial x^2}-l^2\frac{\partial^2}{\partial x^2}\left(D_{11}\frac{\partial^2 w}{\partial x^2}\right)\right)-\frac{\partial}{\partial x}\left(\begin{array}{l}\left(\begin{array}{l}A_{11}\dfrac{\partial u}{\partial x}+\dfrac{1}{2}A_{11}\left(\dfrac{\partial w}{\partial x}\right)^2\\ \qquad\dfrac{\partial^2\left(A_{11}\dfrac{\partial u}{\partial x}+\dfrac{1}{2}A_{11}\left(\dfrac{\partial w}{\partial x}\right)^2\right)}{\partial x^2}\\ -l^2\end{array}\right)\dfrac{\partial w}{\partial x}\end{array}\right)\\ &+(ea)^2\frac{\partial^2}{\partial x^2}\left(\frac{\partial}{\partial x}\left(\left(\left(A_{11}\frac{\partial u}{\partial x}+\frac{1}{2}A_{11}\left(\frac{\partial w}{\partial x}\right)^2-l^2\frac{\partial^2}{\partial x^2}\left(A_{11}\frac{\partial u}{\partial x}+\frac{1}{2}A_{11}\left(\frac{\partial w}{\partial x}\right)^2\right)\right)\right)\frac{\partial w}{\partial x}\right)\right)\\ &=+m_0\frac{\partial^2 w}{\partial t^2}-m_1\frac{\partial^4 w}{\partial x^2\partial t^2}-(ea)^2\frac{\partial^2}{\partial x^2}\left(m_0\frac{\partial^2 w}{\partial t^2}-m_1\frac{\partial^4 w}{\partial x^2\partial t^2}\right)\end{aligned} \tag{21a}$$

δw:

$$
\begin{aligned}
&D_{11}\frac{\partial^4 w}{\partial x^4}+2\frac{dD_{11}}{dx}\frac{\partial^3 w}{\partial x^3}+\frac{d^2D_{11}}{dx^2}\frac{\partial^2 w}{\partial x^2}-l^2\left(D_{11}\frac{\partial^6 w}{\partial x^6}+\frac{d^4D_{11}}{dx^4}\frac{\partial^2 w}{\partial x^2}+6\frac{d^2D_{11}}{dx^2}\frac{\partial^4 w}{\partial x^4}+4\left(\frac{d^3D_{11}}{dx^3}\frac{\partial^3 w}{\partial x^3}+\frac{dD_{11}}{dx}\frac{\partial^5 w}{\partial x^5}\right)\right)\\
&-\frac{dA_{11}}{dx}\frac{\partial u}{\partial x}-A_{11}\frac{\partial^2 u}{\partial x^2}-\left(\frac{1}{2L}\frac{dA_{11}}{dx}\int_0^L\left(\frac{\partial w}{\partial x}\right)^2dx+\frac{1}{L}A_{11}\int_0^L\frac{\partial^2 w}{\partial x^2}\frac{\partial w}{\partial x}dx\right)\frac{\partial w}{\partial x}-\frac{1}{2L}A_{11}\int_0^L\left(\frac{\partial w}{\partial x}\right)^2dx\,\frac{\partial^2 w}{\partial x^2}\\
&+l^2\left[\begin{array}{l}\left(\begin{array}{l}\frac{1}{2L}\frac{d^3A_{11}}{dx^3}\int_0^L\left(\frac{\partial w}{\partial x}\right)^2dx+\frac{3}{L}\frac{d^2A_{11}}{dx^2}\int_0^L\frac{\partial^2 w}{\partial x^2}\frac{\partial w}{\partial x}dx+\frac{3}{L}\frac{dA_{11}}{dx}\int_0^L\frac{\partial^3 w}{\partial x^3}\frac{\partial w}{\partial x}dx+\frac{d^3A_{11}}{dx^3}\frac{\partial u}{\partial x}+3\frac{d^2A_{11}}{dx^2}\frac{\partial^2 u}{\partial x^2}\\+3\frac{dA_{11}}{dx}\frac{\partial^3 u}{\partial x^3}+A_{11}\frac{\partial^4 u}{\partial x^4}+\frac{3}{L}\frac{dA_{11}}{dx}\int_0^L\left(\frac{\partial^2 w}{\partial x^2}\right)^2dx+\frac{3}{L}A_{11}\int_0^L\frac{\partial^3 w}{\partial x^3}\frac{\partial^2 w}{\partial x^2}dx+\frac{1}{L}A_{11}\int_0^L\frac{\partial^4 w}{\partial x^4}\frac{\partial w}{\partial x}dx\end{array}\right)\frac{\partial w}{\partial x}\\+\left(\frac{1}{2L}\frac{d^2A_{11}}{dx^2}\int_0^L\left(\frac{\partial w}{\partial x}\right)^2dx+\frac{2}{L}\frac{dA_{11}}{dx}\int_0^L\frac{\partial^2 w}{\partial x^2}\frac{\partial w}{\partial x}dx+\frac{1}{L}A_{11}\int_0^L\frac{\partial^3 w}{\partial x^3}\frac{\partial w}{\partial x}dx+\frac{1}{L}A_{11}\int_0^L\left(\frac{\partial^2 w}{\partial x^2}\right)^2dx+\frac{d^2A_{11}}{dx^2}\frac{\partial u}{\partial x}+2\frac{dA_{11}}{dx}\frac{\partial^2 u}{\partial x^2}+A_{11}\frac{\partial^3 u}{\partial x^3}\right)\frac{\partial^2 w}{\partial x^2}\end{array}\right]\\
&+(ea)^2\left[\begin{array}{l}\left(\begin{array}{l}\frac{1}{2L}\frac{d^3A_{11}}{dx^3}\int_0^L\left(\frac{\partial w}{\partial x}\right)^2dx+\frac{3}{L}\frac{d^2A_{11}}{dx^2}\int_0^L\frac{\partial^2 w}{\partial x^2}\frac{\partial w}{\partial x}dx+\frac{3}{L}\frac{dA_{11}}{dx}\int_0^L\frac{\partial^3 w}{\partial x^3}\frac{\partial w}{\partial x}dx+\frac{3}{L}\frac{dA_{11}}{dx}\int_0^L\left(\frac{\partial^2 w}{\partial x^2}\right)^2dx\\+\frac{3}{L}A_{11}\int_0^L\frac{\partial^3 w}{\partial x^3}\frac{\partial^2 w}{\partial x^2}dx+\frac{1}{L}A_{11}\int_0^L\frac{\partial^4 w}{\partial x^4}\frac{\partial w}{\partial x}dx+\frac{d^3A_{11}}{dx^3}\frac{\partial u}{\partial x}+3\frac{d^2A_{11}}{dx^2}\frac{\partial^2 u}{\partial x^2}+3\frac{dA_{11}}{dx}\frac{\partial^3 u}{\partial x^3}+A_{11}\frac{\partial^4 u}{\partial x^4}\end{array}\right)\frac{\partial w}{\partial x}\\+3\left(\begin{array}{l}\frac{1}{2L}\frac{d^2A_{11}}{dx^2}\int_0^L\left(\frac{\partial w}{\partial x}\right)^2dx+\frac{2}{L}\frac{dA_{11}}{dx}\int_0^L\frac{\partial^2 w}{\partial x^2}\frac{\partial w}{\partial x}dx+2\left(\frac{d^2A_{11}}{dx^2}\frac{\partial u}{\partial x}+2\frac{dA_{11}}{dx}\frac{\partial^2 u}{\partial x^2}+A_{11}\frac{\partial^3 u}{\partial x^3}\right)\\+\frac{1}{L}A_{11}\int_0^L\frac{\partial^3 w}{\partial x^3}\frac{\partial w}{\partial x}dx+\frac{1}{L}A_{11}\int_0^L\left(\frac{\partial^2 w}{\partial x^2}\right)^2dx+\left(\frac{1}{2L}A_{11}\int_0^L\left(\frac{\partial w}{\partial x}\right)^2dx+A_{11}\frac{\partial u}{\partial x}\right)\frac{\partial^4 w}{\partial x^4}\end{array}\right)\frac{\partial^2 w}{\partial x^2}+3\left(\begin{array}{l}\frac{1}{2L}\frac{dA_{11}}{dx}\int_0^L\left(\frac{\partial w}{\partial x}\right)^2dx\\+\frac{1}{L}A_{11}\int_0^L\frac{\partial^2 w}{\partial x^2}\frac{\partial w}{\partial x}dx\\+3\left(\frac{dA_{11}}{dx}\frac{\partial u}{\partial x}+A_{11}\frac{\partial^2 u}{\partial x^2}\right)\end{array}\right)\frac{\partial^3 w}{\partial x^3}\end{array}\right]\\
&-l^2(ea)^2\left[\begin{array}{l}\left(\begin{array}{l}\frac{1}{2L}\frac{d^5A_{11}}{dx^5}\int_0^L\left(\frac{\partial w}{\partial x}\right)^2dx+\frac{5}{L}\frac{d^4A_{11}}{dx^4}\int_0^L\frac{\partial^2 w}{\partial x^2}\frac{\partial w}{\partial x}dx+\frac{10}{L}\frac{d^3A_{11}}{dx^3}\int_0^L\frac{\partial^3 w}{\partial x^3}\frac{\partial w}{\partial x}dx+\frac{4}{L}\frac{d^3A_{11}}{dx^3}\int_0^L\left(\frac{\partial^2 w}{\partial x^2}\right)^2dx+\frac{10}{L}\frac{d^2A_{11}}{dx^2}\int_0^L\frac{\partial^4 w}{\partial x^4}\frac{\partial w}{\partial x}dx\\+\frac{30}{L}\frac{d^2A_{11}}{dx^2}\int_0^L\frac{\partial^3 w}{\partial x^3}\frac{\partial^2 w}{\partial x^2}dx+\frac{6}{L}\frac{d^3A_{11}}{dx^3}\int_0^L\left(\frac{\partial^2 w}{\partial x^2}\right)^2dx+\frac{5}{L}\frac{dA_{11}}{dx}\int_0^L\frac{\partial^5 w}{\partial x^5}\frac{\partial w}{\partial x}dx+\frac{20}{L}\frac{dA_{11}}{dx}\int_0^L\frac{\partial^4 w}{\partial x^4}\frac{\partial^2 w}{\partial x^2}dx+\frac{15}{L}\frac{dA_{11}}{dx}\int_0^L\left(\frac{\partial^3 w}{\partial x^3}\right)^2dx\\+\frac{10}{L}A_{11}\int_0^L\frac{\partial^4 w}{\partial x^4}\frac{\partial^3 w}{\partial x^3}dx+\frac{5}{L}A_{11}\int_0^L\frac{\partial^5 w}{\partial x^5}\frac{\partial^2 w}{\partial x^2}dx+\frac{1}{L}A_{11}\int_0^L\frac{\partial^6 w}{\partial x^6}\frac{\partial w}{\partial x}dx+\frac{d^5A_{11}}{dx^5}\frac{\partial u}{\partial x}+5\frac{d^4A_{11}}{dx^4}\frac{\partial^2 u}{\partial x^2}+10\frac{d^3A_{11}}{dx^3}\frac{\partial^3 u}{\partial x^3}\\+10\frac{d^2A_{11}}{dx^2}\frac{\partial^4 u}{\partial x^4}+5\frac{dA_{11}}{dx}\frac{\partial^5 u}{\partial x^5}+A_{11}\frac{\partial^6 u}{\partial x^6}\end{array}\right)\frac{\partial w}{\partial x}\\+3\left(\begin{array}{l}\frac{1}{2L}\frac{d^4A_{11}}{dx^4}\int_0^L\left(\frac{\partial w}{\partial x}\right)^2dx+\frac{4}{L}\frac{d^3A_{11}}{dx^3}\int_0^L\frac{\partial^2 w}{\partial x^2}\frac{\partial w}{\partial x}dx+\frac{6}{L}\frac{d^2A_{11}}{dx^2}\int_0^L\frac{\partial^3 w}{\partial x^3}\frac{\partial w}{\partial x}dx+\frac{6}{L}\frac{d^2A_{11}}{dx^2}\int_0^L\left(\frac{\partial^2 w}{\partial x^2}\right)^2dx+\frac{4}{L}\frac{dA_{11}}{dx}\int_0^L\frac{\partial^4 w}{\partial x^4}\frac{\partial w}{\partial x}dx\\+\frac{12}{L}\frac{dA_{11}}{dx}\int_0^L\frac{\partial^3 w}{\partial x^3}\frac{\partial^2 w}{\partial x^2}dx+\frac{3}{L}A_{11}\int_0^L\left(\frac{\partial^3 w}{\partial x^3}\right)^2dx+\frac{4}{L}A_{11}\int_0^L\frac{\partial^4 w}{\partial x^4}\frac{\partial^2 w}{\partial x^2}dx+\frac{1}{L}A_{11}\int_0^L\frac{\partial^5 w}{\partial x^5}\frac{\partial w}{\partial x}dx\\+3\left(\frac{d^4A_{11}}{dx^4}\frac{\partial u}{\partial x}+4\frac{d^3A_{11}}{dx^3}\frac{\partial^2 u}{\partial x^2}+6\frac{d^2A_{11}}{dx^2}\frac{\partial^3 u}{\partial x^3}+4\frac{dA_{11}}{dx}\frac{\partial^4 u}{\partial x^4}+A_{11}\frac{\partial^5 u}{\partial x^5}\right)\end{array}\right)\frac{\partial^2 w}{\partial x^2}\\+3\left(\begin{array}{l}\frac{1}{2L}\frac{d^3A_{11}}{dx^3}\int_0^L\left(\frac{\partial w}{\partial x}\right)^2dx+\frac{3}{L}\frac{d^2A_{11}}{dx^2}\int_0^L\frac{\partial^2 w}{\partial x^2}\frac{\partial w}{\partial x}dx+\frac{3}{L}\frac{dA_{11}}{dx}\int_0^L\frac{\partial^3 w}{\partial x^3}\frac{\partial w}{\partial x}dx+\frac{3}{L}\frac{dA_{11}}{dx}\int_0^L\left(\frac{\partial^2 w}{\partial x^2}\right)^2dx\\+\frac{3}{L}A_{11}\int_0^L\frac{\partial^3 w}{\partial x^3}\frac{\partial^2 w}{\partial x^2}dx+\frac{1}{L}A_{11}\int_0^L\frac{\partial^4 w}{\partial x^4}\frac{\partial w}{\partial x}dx+3\left(\frac{d^3A_{11}}{dx^3}\frac{\partial u}{\partial x}+3\frac{d^2A_{11}}{dx^2}\frac{\partial^2 u}{\partial x^2}+3\frac{dA_{11}}{dx}\frac{\partial^3 u}{\partial x^3}+A_{11}\frac{\partial^4 u}{\partial x^4}\right)\end{array}\right)\frac{\partial^3 w}{\partial x^3}\\+\left(\begin{array}{l}\frac{1}{2L}\frac{d^2A_{11}}{dx^2}\int_0^L\left(\frac{\partial w}{\partial x}\right)^2dx+\frac{2}{L}\frac{dA_{11}}{dx}\int_0^L\frac{\partial^2 w}{\partial x^2}\frac{\partial w}{\partial x}dx+\frac{1}{L}A_{11}\int_0^L\frac{\partial^3 w}{\partial x^3}\frac{\partial w}{\partial x}dx\\+\frac{1}{L}A_{11}\int_0^L\left(\frac{\partial^2 w}{\partial x^2}\right)^2dx+\frac{d^2A_{11}}{dx^2}\frac{\partial u}{\partial x}+2\frac{dA_{11}}{dx}\frac{\partial^2 u}{\partial x^2}+A_{11}\frac{\partial^3 u}{\partial x^3}\end{array}\right)\frac{\partial^4 w}{\partial x^4}\end{array}\right]\\
&=m_0\frac{\partial^2 w}{\partial t^2}-m_1\frac{\partial^4 w}{\partial x^2\partial t^2}-(ea)^2\left(m_0\frac{\partial^4 w}{\partial x^2\partial t^2}+2\frac{dm_0}{dx}\frac{\partial^3 w}{\partial x\,\partial t^2}+\frac{d^2m_0}{dx^2}\frac{\partial^2 w}{\partial t^2}-m_1\frac{\partial^6 w}{\partial x^4\partial t^2}-2\frac{dm_1}{dx}\frac{\partial^5 w}{\partial x^3\partial t^2}-\frac{d^2m_1}{dx^2}\frac{\partial^4 w}{\partial x^2\partial t^2}\right)
\end{aligned}
\tag{21b}
$$

3. Solution methodology

To get the findings, the numerical technique (GDQM) is utilized. In GDQM, the r-th order derivative of a function is is defined as follows (Azimi *et al*. 2016, Ghadiri *et al*. 2016a, b, c, d, 2017a, b, c, d, Ghadiri and Shafiei 2016a, b, c, Shafiei *et al*. 2016a, b, c, d, e, f, g, 2017a, b, c, 2019, 2020, Ebrahimi and Shafiei 2017, Ebrahimi *et al*. 2017,

Mirjavadi *et al*. 2017a, b, c, d, Shafiei and Kazemi 2017a, b, Azimi *et al*. 2018, Shafiei and She 2018, Al-Furjan *et al*. 2020a, b, c, 2021a, b, c, d, Huang *et al*. 2021, Shariati *et al*. 2021)

$$\left.\frac{\partial^r f\left(x\right)}{\partial x^{\,r}}\right|_{x=x_p}=\sum_{j=1}^{n}C_{ij}^{(r)}f\left(x_i\right) \tag{22}$$

The number of grid points is specified by the letter 'n,' and C_{ij} as the weighting coefficient is calculated as follows:

$$\begin{aligned} C_{ij}^{(1)}&=\frac{P\left(x_i\right)}{\left(x_i-x_j\right)P\left(x_j\right)}; && \mathrm{i}\neq \mathrm{j}=1,2,...,\mathrm{n}\\ C_{ji}^{(1)}&=-\sum_{i=1,j\neq i}^{n}C_{ji}^{(1)}; && i=j \end{aligned} \tag{23}$$

where $P(x)$ is:

$$P\left(x_i\right)=\prod_{i=1,i\neq j}^{n}\left(x_j-x_i\right) \tag{24}$$

$C^{(r)}$ along the x-axis is calculated as follows:

$$\begin{aligned} C_{iji}^{(r)}&=r\left[C_{ji}^{(r-1)}C_{ji}^{(1)}-\frac{C_{ji}^{(r-1)}}{\left(x_j-x_i\right)}\right]; && j\neq i=1,2,...,n\\ C_{jj}^{(r)}&=-\sum_{i=1,j\neq i}^{n}C_{ji}^{(r)}; && i=j=1,2,...,n \end{aligned} \tag{25}$$

The mesh point distribution is determined using the Chebyshev-Gauss-Lobatto technique as follows:

$$\mathbf{2}x_i=\left(1-\cos\left(\frac{(i-1)}{(N-1)}\pi\right)\right)L \tag{26}$$

Consider the FG nanotube's nonlinear motion equations, which are a composite of the three mass matrices. The following are the linear and nonlinear stiffnesses:

$$\left\{\left[K\right]_{Linear}+\left[K\right]_{Non-linear}-\omega^2\left[M\right]\right\}\left\{\lambda\right\}=0 \tag{27}$$

Additionally, the boundary conditions are composed of three matrices. As a consequence, the following matrix represents the linear stiffness:

$$\left\{\left[K\right]-\omega^2\left[M\right]\right\}\left\{\lambda\right\}=0 \tag{28}$$

To begin, we use the extended differential quadrature method to solve the linear motion equation. After applying the weight coefficients to the linear motion equation, the following result is obtained as below:

We build the matrixes to the boundary and the governing equations while ignoring the nonlinear components. As a result, the basic linear vibration equation of the FG nano-tube is as follows:

$$\begin{bmatrix}\left[K_{dd}\right] & \left[K_{db}\right]\\ \left[K_{bd}\right] & \left[K_{bb}\right]\end{bmatrix}\begin{Bmatrix}\{\lambda_d\}\\ \{\lambda_b\}\end{Bmatrix}=\omega^2\begin{bmatrix}\left[M_{dd}\right] & \left[M_{db}\right]\\ \left[M_{bd}\right] & \left[M_{bb}\right]\end{bmatrix}\begin{Bmatrix}\{\lambda_d\}\\ \{\lambda_b\}\end{Bmatrix} \tag{30}$$

where *d* and *b* correspond to the domain and boundary indices, respectively, and λ denotes the mode form. The nonlinear mode shapes and frequencies are obtained by coupling the nonlinear and linear stiffness matrices with the mass matrix, using the nonlinear stiffness matrix and Eq. (27) as well as the linear mode shape in Eq. (28). Iteration is then utilized to get the nonlinear frequency results by recalculating the frequency to obtain the converged nonlinear frequency (Ghadiri and Shafiei 2016, Shafiei *et al*. 2016a, b, c, d, e, f, g, 2017a, b, c, d, Shafiei and Kazemi 2017, Azimi *et al*. 2018, Hou *et al*. 2021, Huang *et al*. 2021).

$$\begin{aligned} &\frac{dA_{11}(x)}{dx}\left(\sum_{s=1}^{n}C_{rs}^{(1)}u_s+\frac{1}{2}\left(\sum_{s=1}^{n}C_{rs}^{(1)}w_s\right)^2\right)+A_{11}(x)\left(\sum_{s=1}^{n}C_{rs}^{(2)}u_s+\sum_{s=1}^{n}C_{rs}^{(2)}w_s\sum_{s=1}^{n}C_{rs}^{(1)}w_s\right)\\ &-l^2\left[\begin{array}{l}\dfrac{d^3A_{11}(x)}{dx^3}\left(\sum_{s=1}^{n}C_{rs}^{(1)}u_s+\frac{1}{2}\left(\sum_{s=1}^{n}C_{rs}^{(1)}w_s\right)^2\right)\\ +3\dfrac{d^2A_{11}(x)}{dx^2}\left(\sum_{s=1}^{n}C_{rs}^{(2)}u_s+\sum_{s=1}^{n}C_{rs}^{(2)}w_s\sum_{s=1}^{n}C_{rs}^{(1)}w_s\right)\\ +3\dfrac{dA_{11}(x)}{dx}\left(\sum_{s=1}^{n}C_{rs}^{(3)}u_s+\left(\sum_{s=1}^{n}C_{rs}^{(2)}w_s\right)^2+\sum_{s=1}^{n}C_{rs}^{(3)}w_s\sum_{s=1}^{n}C_{rs}^{(1)}w_s\right)\\ +A_{11}(x)\left(\sum_{s=1}^{n}C_{rs}^{(4)}u_s+3\sum_{s=1}^{n}C_{rs}^{(3)}w_s\sum_{s=1}^{n}C_{rs}^{(2)}w_s+\sum_{s=1}^{n}C_{rs}^{(4)}w_s\sum_{s=1}^{n}C_{rs}^{(1)}w_s\right)\end{array}\right]\\ &=\omega^2\left[m_0u_s-(ea)^2\left(m_0\sum_{s=1}^{n}C_{rs}^{(2)}u_s+\frac{\partial^2m_0}{\partial x^2}u_s+2\frac{\partial m_0}{\partial x}\sum_{s=1}^{n}C_{rs}^{(1)}u_s\right)\right] \end{aligned} \tag{29a}$$

$$\begin{aligned} &D_{11}\sum_{s=1}^{n}C_{rs}^{(4)}w_s+2\frac{dD_{11}}{dx}\sum_{s=1}^{n}C_{rs}^{(3)}w_s+\frac{d^2D_{11}}{dx^2}\sum_{s=1}^{n}C_{rs}^{(2)}w_s\\ &-l^2\left[D_{11}\sum_{s=1}^{n}C_{rs}^{(6)}w_s+\frac{d^4D_{11}}{dx^4}\sum_{s=1}^{n}C_{rs}^{(2)}w_s+4\frac{d^3D_{11}}{dx^3}\sum_{s=1}^{n}C_{rs}^{(3)}w_s+4\frac{dD_{11}}{dx}\sum_{s=1}^{n}C_{rs}^{(5)}w_s+6\frac{d^2D_{11}}{dx^2}\sum_{s=1}^{n}C_{rs}^{(4)}w_s\right] \end{aligned} \tag{29b}$$

$$
\begin{aligned}
&-\frac{dA_{11}}{dx}\sum_{s=1}^{n}C_{rs}^{(1)}u_s-\frac{1}{2}\frac{dA_{11}}{dx}\left(\sum_{s=1}^{n}C_{rs}^{(1)}w_s\right)^2-A_{11}\frac{\partial^2 u}{\partial x^2}-A_{11}\sum_{s=1}^{n}C_{rs}^{(1)}w_s\sum_{s=1}^{n}C_{rs}^{(2)}w_s\\
&+(ea)^2\frac{\partial^2}{\partial x^2}\left[\frac{\partial}{\partial x}\left(A_{11}\sum_{s=1}^{n}C_{rs}^{(1)}u_s+\frac{1}{2}A_{11}\left(\sum_{s=1}^{n}C_{rs}^{(1)}w_s\right)^2\right)\sum_{s=1}^{n}C_{rs}^{(1)}w_s\right]\\
&+(l)^2\frac{\partial}{\partial x}\left[\frac{\partial^2}{\partial x^2}\left(A_{11}\sum_{s=1}^{n}C_{rs}^{(1)}u_s+\frac{1}{2}A_{11}\left(\sum_{s=1}^{n}C_{rs}^{(1)}w_s\right)^2\right)\sum_{s=1}^{n}C_{rs}^{(1)}w_s\right]\\
&-(ea)^2(l)^2\frac{\partial^2}{\partial x^2}\left[\frac{\partial}{\partial x}\left(\frac{\partial^2}{\partial x^2}\left(A_{11}\sum_{s=1}^{n}C_{rs}^{(1)}u_s+\frac{1}{2}A_{11}\left(\sum_{s=1}^{n}C_{rs}^{(1)}w_s\right)^2\right)\right)\sum_{s=1}^{n}C_{rs}^{(1)}w_s\right]\\
&=\omega^2\left[m_0w_s-m_1\sum_{s=1}^{n}C_{rs}^{(2)}w_s-(ea)^2\left(\begin{array}{l}m_0\sum_{s=1}^{n}C_{rs}^{(2)}w_s+2\frac{dm_0}{dx}\sum_{s=1}^{n}C_{rs}^{(1)}w_s+\frac{d^2m_0}{dx^2}w_s\\-m_1\sum_{s=1}^{n}C_{rs}^{(4)}w_s-2\frac{dm_1}{dx}\sum_{s=1}^{n}C_{rs}^{(1)}w_s-\frac{d^2m_1}{dx^2}\sum_{s=1}^{n}C_{rs}^{(2)}w_s\end{array}\right)\right]
\end{aligned}
\tag{29b}
$$

Table 2 Comparison of findings for simply-supported Euler-Bernoulli beam theory with Reddy (2007)

	$(ea)^2 = 0$	$(ea)^2 = 0.5$	$(ea)^2 = 1$	$(ea)^2 = 2$	$(ea)^2 = 3$	$(ea)^2 = 4$
Reddy (2007)	9.8696	9.6347	9.4159	9.0195	8.6693	8.3569
Present study	9.8695892819	9.6347583599	9.4159892578	9.0195697277	8.6693506387	8.35692191826

Table 3 The non-dimensional frequency of a nanotube is compared to that of Shafiei and She (2018) for completely clamped nono-beam theory, ($R_o = L/10 = 2R_i$, $\mu_{e0a} = 4\mu_l = 1$)

		Present Euler-Bernoulli theory	Shafiei and She (2018)
First frequency	n = 0	21.62128292	21.58935
	n = 0.25	17.4608717	17.70612
	n = 0.5	15.19437084	15.36206
	n = 0.75	13.83456675	13.92855
	n = 1	12.94944336	12.86888
Second frequency	n = 0	43.63616647	43.42399
	n = 0.25	35.05493773	35.19731
	n = 0.5	30.43092628	30.50317
	n = 0.75	28.13400516	27.79459
	n = 1	25.97828192	25.80996

Table 4 Comparison of the fundamental normalized frequency in different nonlinear amplitude (Amp), for fully clamped and simply-supported beams

	Simply-Supported		Clamped	
	Present Study	Lestari and Hanagud (2001)	Present Study	Malekzadeh and Shojaee (2013)
Amp = 1	1.089155838	1.0892	1.022200907	1.0222
Amp = 2	1.317761785	1.3178	1.085711201	1.0858
Amp = 3	1.625604381	1.6257	1.183187083	1.1823

Table 5 The nonlinear first frequency ($\sqrt{\psi}$) of axially FG nanotubes against size effect parameters, AFG power indices, and rate of cross-section change under various boundary circumstances are investigated (Amp = 1, SUS304/Si_3N_4)

Boundary condition			Local results	$\mu_{ea} = 0.0$, $\mu_l = 0.2$	$\mu_{ea} = 0.2$, $\mu_l = 0.0$
Simply-Supported	Pure SUS304	$\beta_R = -0.25$	2.294709553	2.92939351	2.137977284
		$\beta_R = 0.0$	2.156402508	4.04189011	2.014125209

Table 5 Continued

Boundary condition			Local results	μ_{ea} = 0.0, μ_l = 0.2	μ_{ea} = 0.2, μ_l = 0.0
Simply-Supported	Pure SUS304	β_R = +0.25	2.567708175	2.436230283	2.3828295
Simply Supported-Clamped	Pure SUS304	β_R = -0.25	2.748089635	3.119976509	2.536773492
		β_R = 0.0	2.639723867	2.491311512	2.441268968
		β_R = +0.25	2.567708175	2.436230283	2.3828295
	AFG, n = 1	β_R = -0.25	3.212883719	2.699769009	2.948541819
		β_R = 0.0	3.077768516	2.559195122	2.824406335
		β_R = +0.25	2.989052174	2.576734858	2.745557945
Fully clamped	Pure SUS304	β_R = -0.25	3.383291563	3.104004055	3.101355363
		β_R = 0.0	3.14532407	2.197143468	2.892659873
		β_R = +0.25	2.989451812	2.705024249	2.761343105
	AFG, n = 1	β_R = -0.25	3.993972321	1.213023857	3.668727633
		β_R = 0.0	3.703036773	2.74887766	3.402141914
		β_R = +0.25	3.511185324	2.577104709	3.228557075

Table 6 The nonlinear second frequency ($\sqrt{\psi}$) of axially FG nanotubes against size effect parameters, AFG power indices, and rate of cross-section change under various boundary circumstances are investigated (Amp = 1, SUS304/Si_3N_4)

Boundary condition			Local results	μ_{ea} = 0.0, μ_l = 0.2	μ_{ea} = 0.2, μ_l = 0.0
Simply-Supported	Pure SUS304	β_R = -0.25	4.581352518	4.72391953	3.769083611
		β_R = 0.0	4.312635741	0.283124836	3.594786727
		β_R = +0.25	4.100162794	2.900201601	3.443957362
	AFG, n = 1	β_R = -0.25	5.453827575	1.727065646	4.459986413
		β_R = 0.0	5.100944913	1.374862637	4.216866465
		β_R = +0.25	4.891710744	6.936629554	4.079216256
Simply Supported-Clamped	Pure SUS304	β_R = -0.25	5.064207498	5.635827744	4.102300233
		β_R = 0.0	4.782835174	1.101344212	3.904435179
		β_R = +0.25	4.603414697	1.01272787	3.800179
	AFG, n = 1	β_R = -0.25	5.990887178	1.307680377	4.815056348
		β_R = 0.0	5.63225075	6.662609366	4.551141592
		β_R = +0.25	5.413609436	7.913775222	4.393084865
Fully clamped	Pure SUS304	β_R = -0.25	5.649978044	6.196687638	4.564692032
		β_R = 0.0	5.288451346	2.450360558	4.333465519
		β_R = +0.25	5.017906405	5.529315091	4.159706992
	AFG, n = 1	β_R = -0.25	6.705821392	9.991160685	5.391498397
		β_R = 0.0	6.235086123	3.908752762	5.057268585
		β_R = +0.25	5.934169754	3.408183919	4.860845288

4. Results

Non-dimensional parameters are defined as bellow to understand the results and the results of this study and compare the frequency results to observe the effects of different parameters:

$$Normalized\ Frequency = \frac{Nonlinear\ Frequency}{Linear\ Frequency\ of\ \ perfect\ ceramic\ tube} \quad (31a)$$

$$\psi = \omega\sqrt{\rho_{Ceramic} \times A_{at\ x=0} \times L^4 / E_{Ceramic} \times I_{at\ x=0}} \quad (31b)$$

$$Amp = a\sqrt{I_{at\ x=0} / A_{at\ x=0}} \quad (31c)$$

$$\mu_l = l/L \quad (31d)$$

$$\mu_{ea} = ea/L \quad (31e)$$

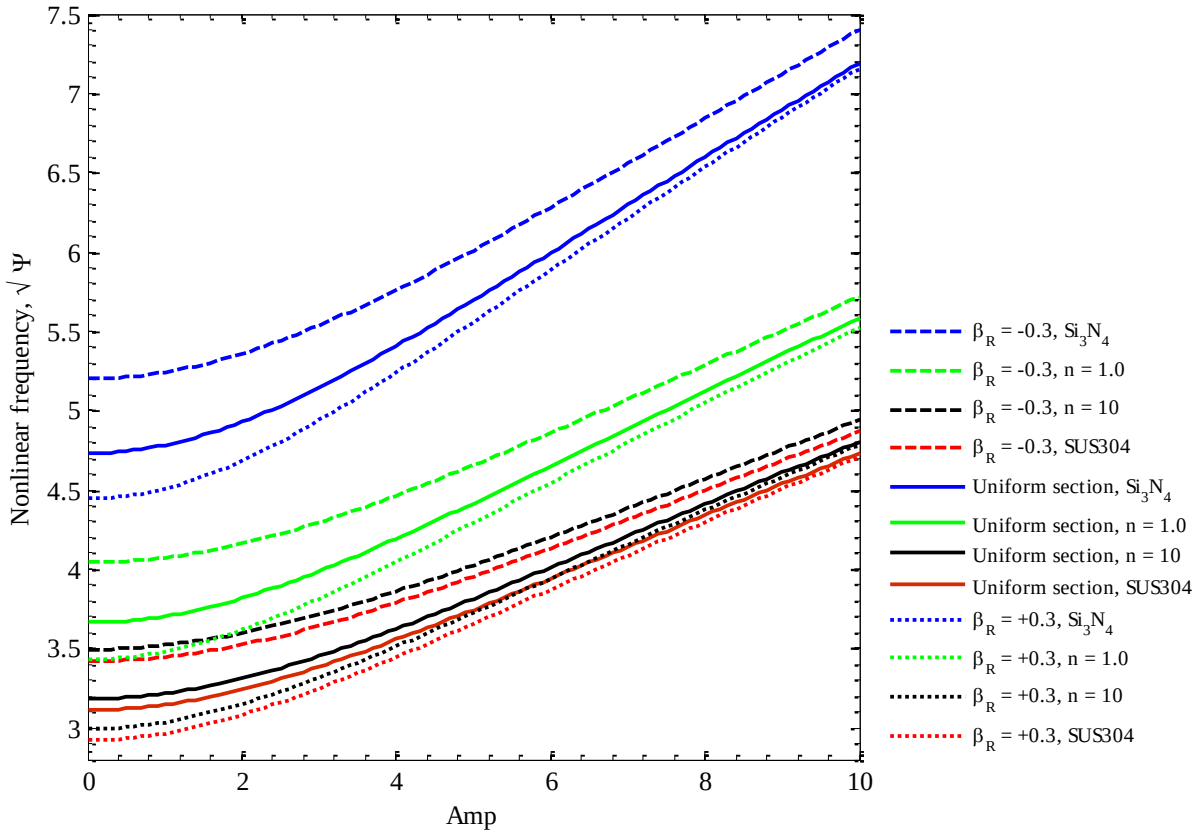

Fig. 2 Fundamental linear (Amp = 0) and nonlinear frequency of clamped nanotube versus Amp, FG power indexes for the various rate of the cross-section, ($SUS304/Si_3N_4$)

Here, ψ, Amp, μ_l and μ_{ea} are the non-dimensional frequency, nonlinear amplitude, non-dimensional gradient strain parameter and non-dimensional nonlocal parameter. The results are compared to the results of Reddy (2007) where in Table 2 where the convergence of the results show the accuracy of the modeling and solving procedure of this study.

Table 3 shows the validation of the following results through comparing the non-dimensional frequency of fully clamped nano-tube with the results of Shafiei and She (2018). This comparison shows the very good validation between the results, while, they are calculated for two different theories.

The validation of present nonlinear results with the result of Lestari and Hanagud (2001) and Malekzadeh and Shojaee (2013) was shown in Table 4. The normalized frequency of fully clamped and simply supported signals for a variety of nonlinear amplitude (Amp) parameters was shown to be very accurate.

Tables 5 and 6 show the nonlinear first and second frequencies of nickel and SUS304 AFG nano-tubes, respectively. Tables 5 Table 6 investigate many parameters such as the nonlocal and strain gradient parameters, the rate of cross-section change, and AFG power indexes for clamped, simply-supported, and clamped-simply supported. These results indicate that the nonlinear frequency increases as the gradient strain parameter and rate of cross-section change (β_R) increase and decrease, respectively, for all boundary conditions. It is also shown that the nonlinear frequency lowers when the nonlocal parameter and AFG power indices increase. This is because the effect of the nonlocal and power indices decreases the influence of material stiffness, resulting in a decrease in nonlinear frequency.

Figs. 2 and 3 shows the effect of nonlinear amplitude parameter (Amp) and the parameter of material distribution on the first two frequencies of tubes, for various rates of cross-section change for simply-supported tubes that are made of metal (SUS304) and ceramic (Si_3N_4). It was displayed that the rate of cross-section (β_R) has a significant effect on the linear and nonlinear frequencies, in such a way that, decrease of β_R increases the frequencies due to this fact that the increment of β_R leads to increase of stiffness of the nano-tube which is the cause of frequency decrement. It is clearly shown increases the AFG power indexes because of the higher stiffness of ceramic than metal tends to decreases the frequency. Moreover, the nonlinear frequency increases with Amp, it's because of the increase of solidity of the tube with the Von-Kármán parameter.

Figs. 4 and 5 explain the porosity impact on the first and second frequency of the tube versus the various AFG parameter (n) on the uniform and nonuniform FG tubes. The porosity tends to enhance the frequency due to the hardening phenomenon, on the other hand, the increment of FG indexes decreases the stiffness and leads to a drop in the frequency in both uniform and nonuniform tubes. Moreover, β_R, as the rate of cross-section change, decreases the frequency because of the softening behavior.

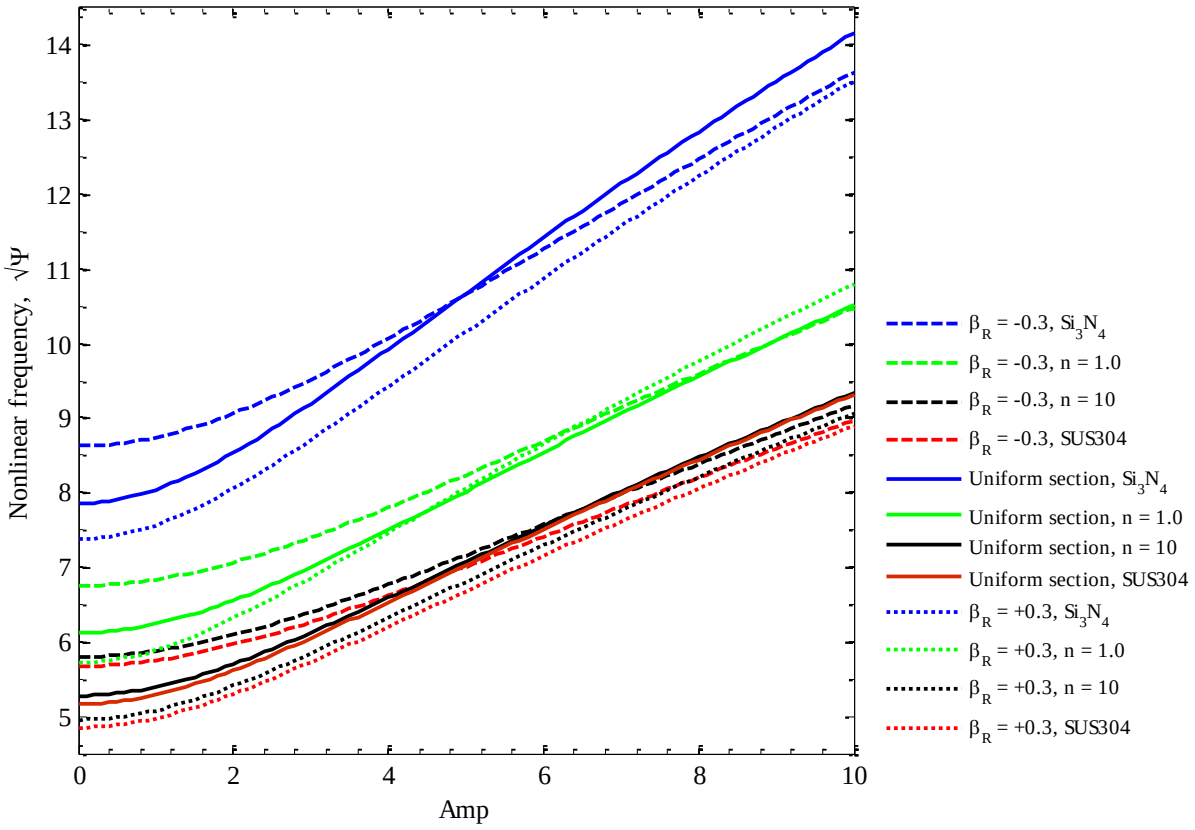

Fig. 3 Second linear (Amp = 0) and nonlinear frequency of clamped nanotube versus Amp, FG power indexes for the various rate of the cross-section, ($SUS304/Si_3N_4$)

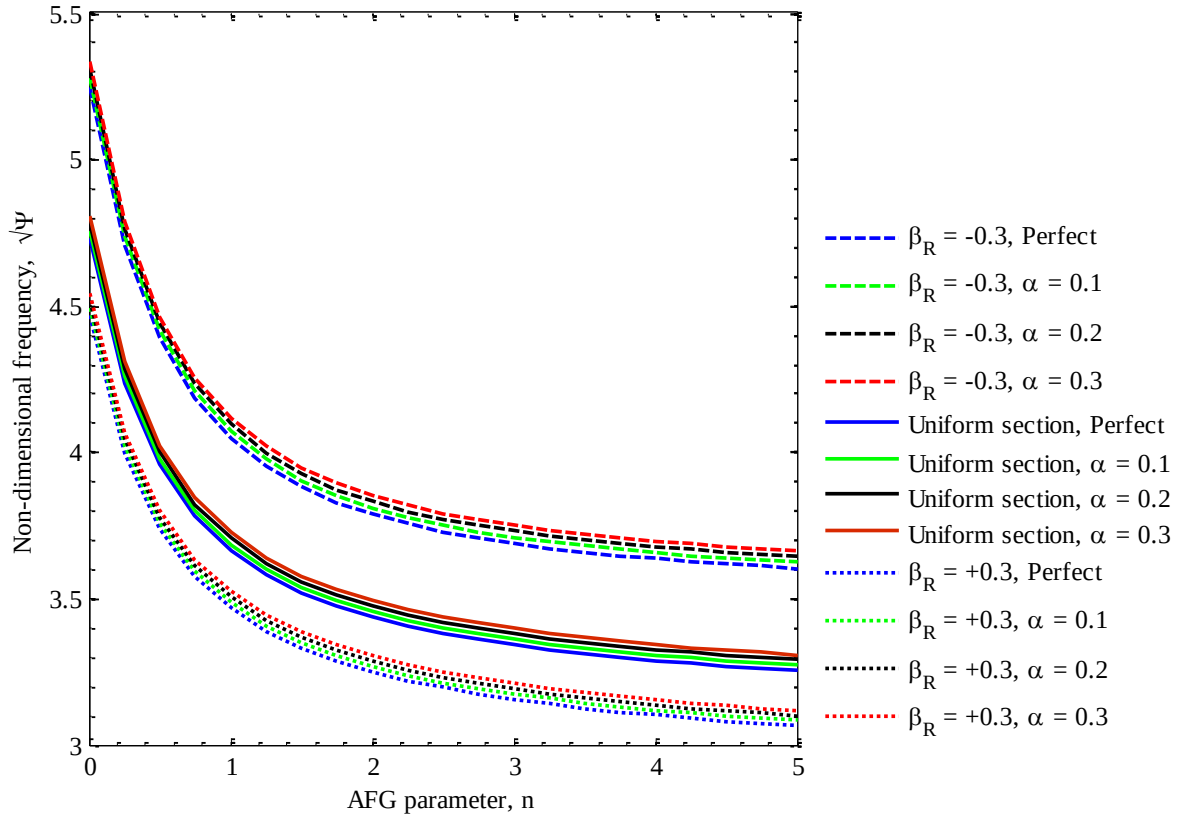

Fig. 4 First frequency of fully clamped nanotube versus AFG power index (n) for the various porosity coefficient (α) and rate of the cross-section (β_R), ($SUS304/Si_3N_4$)

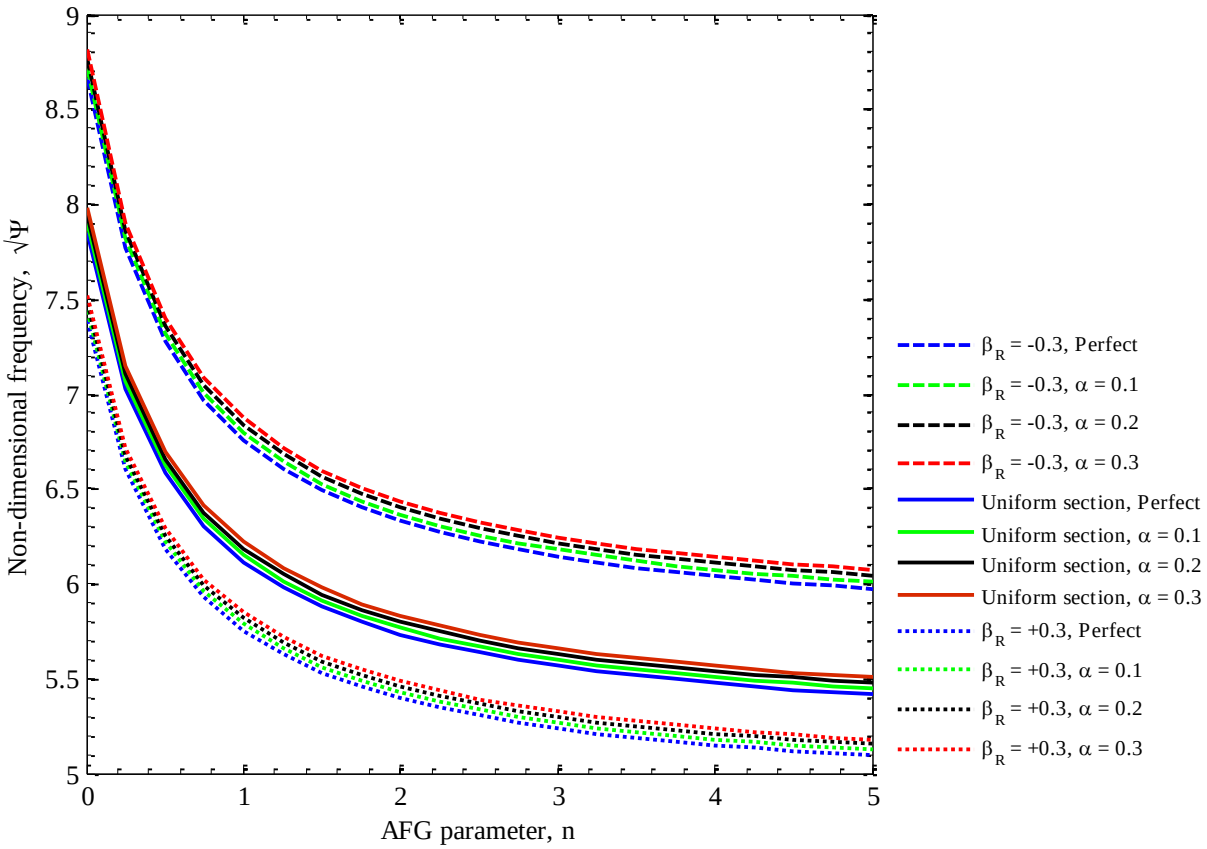

Fig. 5 Second frequency of fully clamped nanotube versus AFG power index (n) for the various porosity coefficient (α) and rate of the cross-section (β_R), (SUS304/Si_3N_4)

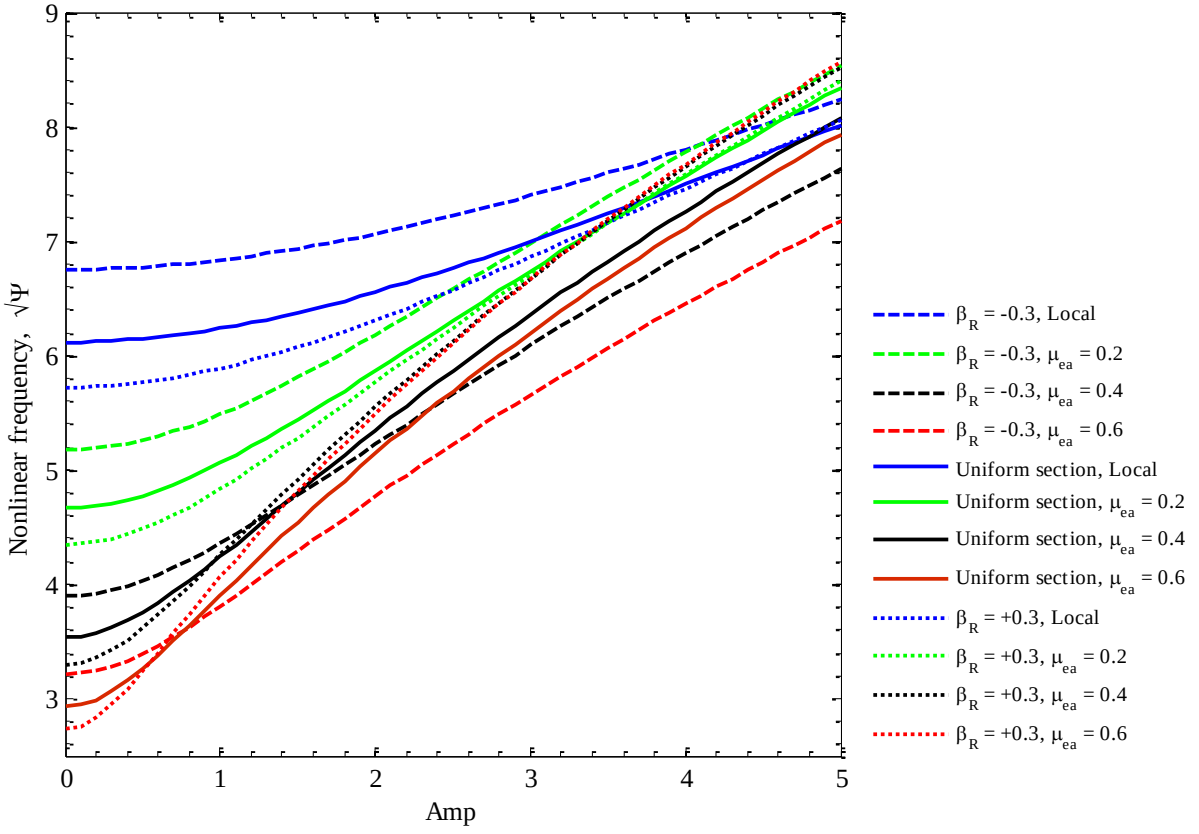

Fig. 6 Fundamental frequency of fully clamped nanotube versus different value of nonlinear amplitude for various parameters of size effect, (β_R = 0.25, n = 1, α = 0.1, SUS304/Si_3N_4)

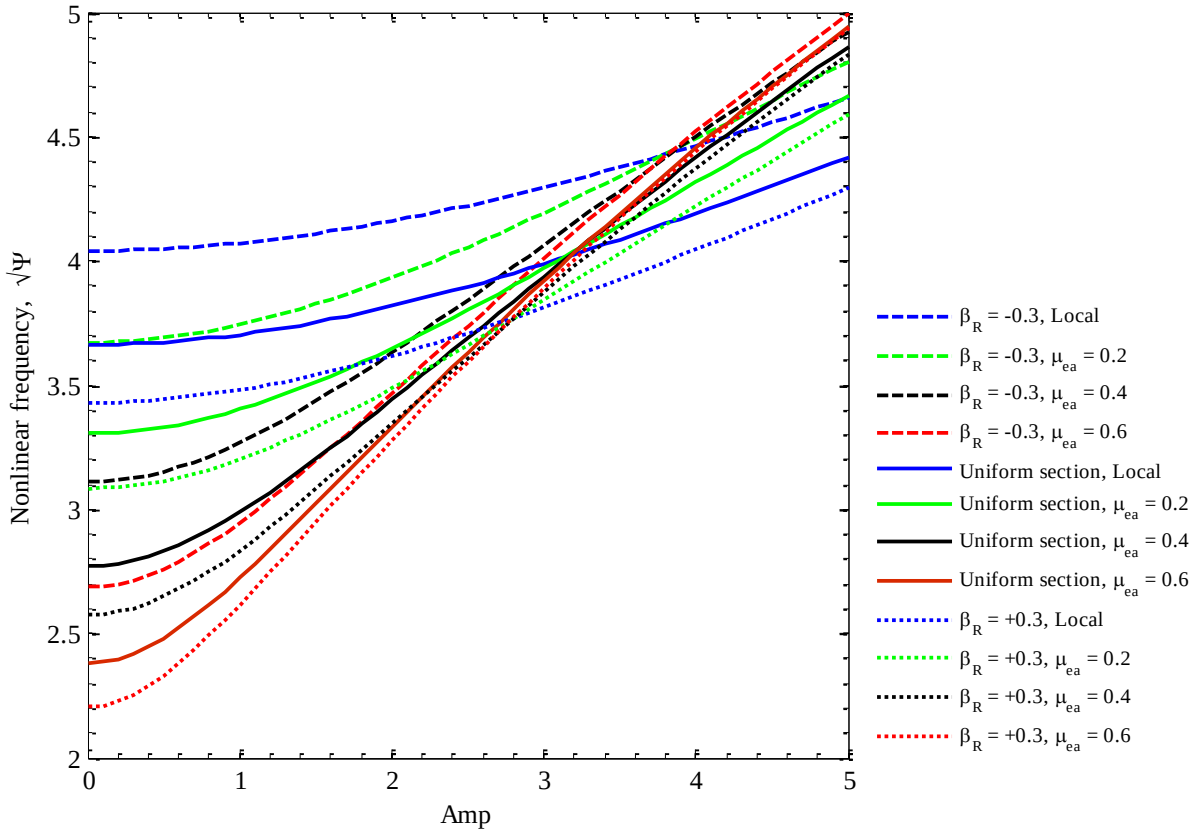

Fig. 7 Second frequency of simply-supported nano-tube versus different value of nonlinear amplitude for various parameters of size effect, (β_R = 0.25, n = 1, α = 0.1, SUS304/Si_3N_4)

Figs. 6 and 7 illustrate the impact of nonlocal factors on the nonlinear first and second frequencies of functionally graded nanotubes as a function of the nonlinear amplitude for both uniform and nonuniform tube sections. Due to the nonlocal parameter's softening effect, both frequencies decrease through the nonlocal parameter, which also lowers the tube stiffness. The nonlinearity of nonlinear amplitude enhances the FG tube's stability and frequency. As previously stated, the cross-section rate (β_R) has a major effect on the dynamic behavior of tubes, and the nonuniformity reduces the stability of FG tubes.

5. Conclusions

In this study, the nonlinear frequency of an axially functionally graded non-uniform nano-tube with porosity is investigated. The Euler-Bernoulli beam model is used to represent the nanotube, and the material composition changes throughout its length. The results in this study are derived utilizing the generalized differential quadrature method, and the nonlocal strain gradient, as well as Eringen's nonlocal theory, are considered. The findings are examined for various nonlinearities, nonlocal and strain gradient parameters, AFG power indices, porosity parameter, and different non-uniformities of the nano-tube for clamped, simply supported, and clamped-simply supported boundary conditions. The main results covered in this research are as follows:

• The frequency increases with nonlinearity for all of the boundary conditions stated.

• As the stiffness increases with the gradient strain parameter, the frequency increases as well.

• The nonlocal parameter, unlike the gradient strain parameter, decreases stiffness and hence frequency.

• The nonlocal and strain gradient parameters have no impact on each other.

• When these parameters are raised, the effect of both nonlocal and strain gradient components increases. To put it another way, the effects of these variables are not linear.

• The frequency decreases as the stiffness decreases, as do the AFG power indices.

• With this kind of porosity, the frequency increases.

• As βR rises, the frequency decreases.

• For clamped, simply supported, and clamped-simply supported boundary conditions, the studied parameters have the same effect.

References

Aifantis, E.C. (1992), "On the role of gradients in the localization of deformation and fracture", *Int. J. Eng. Sci.*, **30**(10), 1279-1299, https://doi.org/10.1016/0020-7225(92)90141-3.

Akbas, S.D. (2018a), "Forced vibration analysis of cracked functionally graded microbeams", *Adv. Nano Res.*, **6**(1), 39-55. http://doi.org/10.12989/anr.2018.6.1.039.

Akbaş, Ş.D. (2018b), "Bending of a cracked functionally graded nanobeam", *Adv. Nano Res.*, **6**(3), 219-242.

http://doi.org/10.12989/anr.2018.6.3.219.

Al-Furjan, M.S.H., Habibi, M., Ni, J., Jung, D.w. and Tounsi, A. (2020a), "Frequency simulation of viscoelastic multi-phase reinforced fully symmetric systems", *Eng. Comput*., 1-17. https://doi.org/10.1007/s00366-020-01200-x.

Al-Furjan, M.S.H., Habibi, M., rahimi, A., Chen, G., Safarpour, H., Safarpour, M. and Tounsi, A. (2020b), "Chaotic simulation of the multi-phase reinforced thermo-elastic disk using GDQM", *Eng*. *Comput*., 1-24. https://doi.org/10.1007/s00366-020-01144-2.

Al-Furjan, M.S.H., Safarpour, H., Habibi, M., Safarpour, M. and Tounsi, A. (2020c), "A comprehensive computational approach for nonlinear thermal instability of the electrically FG-GPLRC disk based on GDQ method", *Eng*. *Comput.*, 1-18. https://doi.org/10.1007/s00366-020-01088-7.

Al-Furjan, M.S.H., Dehini, R., Khorami, M., Habibi, M. and won Jung, D. (2021a), "On the dynamics of the ultra-fast rotating cantilever orthotropic piezoelectric nanodisk based on nonlocal strain gradient theory", *Compos*. *Struct*., **255**, 112990. https://doi.org/10.1016/j.compstruct.2020.112990.

Al-Furjan, M.S.H., Fereidouni, M., Sedghiyan, D., Habibi, M. and Jung, D.W. (2021b), "Three-dimensional frequency response of the CNT-Carbon-Fiber reinforced laminated circular/annular plates under initially stresses", *Compos*. *Struct*., **257**, 113146. https://doi.org/10.1016/j.compstruct.2020.113146.

Al-Furjan, M.S.H., Habibi, M., Ghabussi, A., Safarpour, H., Safarpour, M. and Tounsi, A. (2021c), "Non-polynomial framework for stress and strain response of the FG-GPLRC disk using three-dimensional refined higher-order theory", *Eng*. *Struct*., **228**, 111496. https://doi.org/10.1016/j.engstruct.2020.111496.

Al-Furjan, M.S.H., hatami, A., Habibi, M., Shan, L. and Tounsi, A. (2021d), "On the vibrations of the imperfect sandwich higher-order disk with a lactic core using generalize differential quadrature method", *Compos*. *Struct*., **257**, 113150. https://doi.org/10.1016/j.compstruct.2020.113150.

Alibeigloo, A. and Emtehani, A. (2015), "Static and free vibration analyses of carbon nanotube-reinforced composite plate using differential quadrature method", *Meccanica*. **50**(1), 61-76. https://doi.org/10.1007/s11012-014-0050-7.

Allahkarami, F., Nikkhah-Bahrami, M. and Saryazdi, M.G. (2017), "Damping and vibration analysis of viscoelastic curved microbeam reinforced with FG-CNTs resting on viscoelastic medium using strain gradient theory and DQM", *Steel Compos*. *Struct*., **25**(2), 141-155. https://doi.org/10.12989/scs.2017.25.2.141.

Arefi, M. and Zenkour, A.M. (2018), "Free vibration analysis of a three-layered microbeam based on strain gradient theory and three-unknown shear and normal deformation theory", *Steel Compos*. *Struct*., **26**(4), 421-437. https://doi.org/10.12989/scs.2018.26.4.421.

Arshid, E., Khorasani, M., Soleimani-Javid, Z., Amir, S. and Tounsi, A. (2021), "Porosity-dependent vibration analysis of FG microplates embedded by polymeric nanocomposite patches considering hygrothermal effect via an innovative plate theory", *Eng*. *Comput*., 1-22. http://doi.org/10.1007/s00366-021-01382-y.

Aydogdu, M., Arda, M. and Filiz, S. (2018), "Vibration of axially functionally graded nano rods and beams with a variable nonlocal parameter", *Adv. Nano Res*., **6**(3), 257-278. http://doi.org/10.12989/anr.2018.6.3.257.

Azimi, M., Mirjavadi, S.S., Shafiei, N. and Hamouda, A.M.S. (2016), "Thermo-mechanical vibration of rotating axially functionally graded nonlocal Timoshenko beam", *Appl*. *Phys*. *A*., **123**(1), 104, http://doi.org/10.1007/s00339-016-0712-5.

Azimi, M., Mirjavadi, S.S., Shafiei, N., Hamouda, A.M.S. and Davari, E. (2018), "Vibration of rotating functionally graded Timoshenko nano-beams with nonlinear thermal distribution", *Mech*. *Adv*. *Mater*. *Struct*., **25**(6), 467-480, http://doi.org/10.1080/15376494.2017.1285455.

Bai, Y., Alzahrani, B., Baharom, S. and Habibi, M. (2020), "Semi-numerical simulation for vibrational responses of the viscoelastic imperfect annular system with honeycomb core under residual pressure", *Eng*. *Comput*., 1-26. http://doi.org/10.1007/s00366-020-01191-9.

Bekkaye, T.H.L., Fahsi, B., Bousahla, A.A., Bourada, F., Tounsi, A., Benrahou, K.H., Tounsi, A. and Al-Zahrani, M.M. (2020), "Porosity-dependent mechanical behaviors of FG plate using refined trigonometric shear deformation theory", *Comput. Concrete*., **26**(5), 439-450. https://doi.org/10.12989/cac.2020.26.5.439.

Bellifa, H., Selim, M.M., Chikh, A., Bousahla, A.A., Bourada, F., Tounsi, A., Benrahou, K.H., Al-Zahrani, M.M. and Tounsi, A. (2021), "Influence of porosity on thermal buckling behavior of functionally graded beams", *Smart Struct*. *Syst*., **27**(4), 719-728. http://doi.org/10.12989/sss.2021.27.4.719.

Bensaid, I., Bekhadda, A. and Kerboua, B. (2018), "Dynamic analysis of higher order shear-deformable nanobeams resting on elastic foundation based on nonlocal strain gradient theory", *Adv. Nano Res*., **6**(3), 279-298. http://doi.org/10.12989/anr.2018.6.3.279.

Besseghier, A., Heireche, H., Bousahla, A.A., Tounsi, A. and Benzair, A. (2015), "Nonlinear vibration properties of a zigzag single-walled carbon nanotube embedded in a polymer matrix", *Adv. Nano Res*., **3**(1), 29-37. http://doi.org/10.12989/anr.2015.3.1.029.

Dai, Z., Jiang, Z., Zhang, L. and Habibi, M. (2021a), "Frequency characteristics and sensitivity analysis of a size-dependent laminated nanoshell", *Adv*. *Nano Res*., **10**(2), 175-189. http://doi.org/10.12989/anr.2021.10.2.175.

Dai, Z., Zhang, L., Bolandi, S.Y. and Habibi, M. (2021b), "On the vibrations of the non-polynomial viscoelastic composite open-type shell under residual stresses", *Compos*. *Struct*., **263**, 113599. https://doi.org/10.1016/j.compstruct.2021.113599.

Ebrahimi, F. and Nasirzadeh, P. (2015), "A nonlocal Timoshenko beam theory for vibration analysis of thick nanobeams using differential transform method", *J*. *Theor*. *Appl*. *Mech*., **53**(4), 1041-1052. https://doi.org/10.15632/jtam-pl.53.4.1041.

Ebrahimi, F. and Shafiei, N. (2017), "Influence of initial shear stress on the vibration behavior of single-layered graphene sheets embedded in an elastic medium based on Reddy's higher-order shear deformation plate theory", *Mech*. *Adv*. *Mater*. *Struct*., **24**(9), 761-772. https://doi.org/10.1080/15376494.2016.1196781.

Ebrahimi, F., Shafiei, N., Kazemi, M. and Mousavi Abdollahi, S.M. (2017), "Thermo-mechanical vibration analysis of rotating nonlocal nanoplates applying generalized differential quadrature method", *Mech*. *Adv*. *Mater*. *Struct*., **24**(15), 1257-1273. http://doi.org/10.1080/15376494.2016.1227499.

Ebrahimi, F., Kokaba, M., Shaghaghi, G. and Selvamani, R. (2020), "Dynamic characteristics of hygro-magneto-thermo-electrical nanobeam with non-ideal boundary conditions", *Adv*. *Nano Res*., **8**(2), 169-182. https://doi.org/10.12989/anr.2020.8.2.169.

Ehyaei, J., Akbarshahi, A. and Shafiei, N. (2017), "Influence of porosity and axial preload on vibration behavior of rotating FG nanobeam", *Adv. Nano Res*., **5**(2), 141-169. http://doi.org/10.12989/anr.2017.5.2.141.

Eringen, A.C. (1983), "On differential equations of nonlocal elasticity and solutions of screw dislocation and surface waves", *J*. *Appl*. *Phys*., **54**(9), 4703-4710. http://doi.org/10.1063/1.332803.

Filiz, S. and Aydogdu, M. (2015), "Wave propagation analysis of

embedded (coupled) functionally graded nanotubes conveying fluid", *Compos. Struct.*, **132** 1260-1273. https://doi.org/10.1016/j.compstruct.2015.07.043.

Gafour, Y., Hamidi, A., Benahmed, A., Zidour, M. and Bensattalah, T. (2020), "Porosity-dependent free vibration analysis of FG nanobeam using non-local shear deformation and energy principle", *Adv. Nano Res.*, **8**(1), 37-47. https://doi.org/10.12989/anr.2020.8.1.037.

Ghadiri, M. and Shafiei, N. (2016a), "Nonlinear bending vibration of a rotating nanobeam based on nonlocal Eringen's theory using differential quadrature method", *Microsyst. Technol.*, **22**(12), 2853-2867. https://doi.org/10.1007/s00542-015-2662-9.

Ghadiri, M. and Shafiei, N. (2016b), "Vibration analysis of a nano-turbine blade based on Eringen nonlocal elasticity applying the differential quadrature method", *J. Vib. Control.*, **23**(19), 3247-3265. https://doi.org/10.1177/1077546315627723.

Ghadiri, M. and Shafiei, N. (2016c), "Vibration analysis of rotating functionally graded Timoshenko microbeam based on modified couple stress theory under different temperature distributions", *Acta Astronautica*, **121**, 221-240. https://doi.org/10.1016/j.actaastro.2016.01.003.

Ghadiri, M., Hosseini, S.H.S. and Shafiei, N. (2016a), "A power series for vibration of a rotating nanobeam with considering thermal effect", *Mech. Adv. Mater. Struct.*, **23**(12), 1414-1420, https://doi.org/10.1080/15376494.2015.1091527.

Ghadiri, M., Shafiei, N. and Akbarshahi, A. (2016b), "Influence of thermal and surface effects on vibration behavior of nonlocal rotating Timoshenko nanobeam", *Appl. Phys. A*, **122**(7), 673. https://doi.org/10.1007/s00339-016-0196-3.

Ghadiri, M., Shafiei, N. and Alireza Mousavi, S. (2016d), "Vibration analysis of a rotating functionally graded tapered microbeam based on the modified couple stress theory by DQEM", *Applied Physics A*, **122**(9), 837. https://doi.org/10.1007/s00339-016-0364-5.

Ghadiri, M., Mahinzare, M., Shafiei, N. and Ghorbani, K. (2017a), "On size-dependent thermal buckling and free vibration of circular FG Microplates in thermal environments", *Microsyst. Technol.*, **23**(10), 4989-5001. https://doi.org/10.1007/s00542-017-3308-x.

Ghadiri, M., Shafiei, N. and Alavi, H. (2017b), "Thermo-mechanical vibration of orthotropic cantilever and propped cantilever nanoplate using generalized differential quadrature method", *Mech. Adv. Mater. Struct.*, **24**(8), 636-646. https://doi.org/10.1080/15376494.2016.1196770.

Ghadiri, M., Shafiei, N. and Babaei, R. (2017c), "Vibration of a rotary FG plate with consideration of thermal and Coriolis effects", *Steel Compos. Struct.*, **25**(2), 197-207. https://doi.org/10.12989/SCS.2017.25.2.197.

Ghadiri, M., Shafiei, N. and Safarpour, H. (2017d), "Influence of surface effects on vibration behavior of a rotary functionally graded nanobeam based on Eringen's nonlocal elasticity", *Microsyst. Technol.*, **23**(4), 1045-1065. https://doi.org/10.1007/s00542-016-2822-6.

Guellil, M., Saidi, H., Bourada, F., Bousahla, A.A., Tounsi, A., Al-Zahrani, M.M., Hussain, M. and Mahmoud, S. (2021), "Influences of porosity distributions and boundary conditions on mechanical bending response of functionally graded plates resting on Pasternak foundation", *Steel Compos. Struct.*, **38**(1), 1-15. http://doi.org/10.12989/scs.2021.38.1.001.

Guo, Y., Mi, H. and Habibi, M. (2021), "Electromechanical energy absorption, resonance frequency, and low-velocity impact analysis of the piezoelectric doubly curved system", *Mech. Syst. Signal Pr.*, **157**, 107723. https://doi.org/10.1016/j.ymssp.2021.107723.

Habibi, M., Darabi, R., Sa, J.C.D. and Reis, A. (2021), "An innovation in finite element simulation via crystal plasticity assessment of grain morphology effect on sheet metal formability", **235**(8), 1937-1951. https://doi.org/10.1177/14644207211024686.

Hadji, L., Madan, R., Bhowmick, S. and Tounsi, A. (2021), "A n-order refined theory for free vibration of sandwich beams with functionally graded porous layers", *Struct. Eng. Mech.*, **79**(3), 279-288., http://doi.org/10.12989/sem.2021.79.3.279.

Hamidi, A., Houari, M.S.A., Mahmoud, S. and Tounsi, A. (2015), "A sinusoidal plate theory with 5-unknowns and stretching effect for thermomechanical bending of functionally graded sandwich plates", *Steel Compos. Struct.*, **18**(1), 235-253. https://doi.org/10.12989/scs.2015.18.1.235.

Hou, F., Wu, S., Moradi, Z. and Shafiei, N. (2021), "The computational modeling for the static analysis of axially functionally graded micro-cylindrical imperfect beam applying the computer simulation", *Eng. Comput.*, 1-19. https://doi.org/10.1007/s00366-021-01456-x.

Hu, J., Ye, C., Ding, Y., Tang, J. and Liu, S. (2021), "A distributed MPC to exploit reactive power V2G for real-time voltage regulation in distribution networks", *IEEE T. Smart Grid*, 1-1. https://doi.org/10.1109/TSG.2021.3109453.

Huang, X., Hao, H., Oslub, K., Habibi, M. and Tounsi, A. (2021a), "Dynamic stability/instability simulation of the rotary size-dependent functionally graded microsystem", *Eng. Comput.*, 1-17. https://doi.org/10.1007/s00366-021-01399-3.

Huang, X., Zhang, Y., Moradi, Z. and Shafiei, N. (2021b), "Computer simulation via a couple of homotopy perturbation methods and the generalized differential quadrature method for nonlinear vibration of functionally graded non-uniform micro-tube", *Eng. Comput.*, 1-18. https://doi.org/10.1007/s00366-021-01395-7.

Huang, X., Zhu, Y., Vafaei, P., Moradi, Z. and Davoudi, M. (2021c), "An iterative simulation algorithm for large oscillation of the applicable 2D-electrical system on a complex nonlinear substrate", *Eng. Comput.*, 1-13. https://doi.org/10.1007/s00366-021-01320-y.

Huo, J., Zhang, G., Ghabussi, A. and Habibi, M. (2021), "Bending analysis of FG-GPLRC axisymmetric circular/annular sector plates by considering elastic foundation and horizontal friction force using 3D-poroelasticity theory", *Compos. Struct.*, **276**, 114438. https://doi.org/10.1016/j.compstruct.2021.114438.

Jiao, J., Ghoreishi, S.-m., Moradi, Z. and Oslub, K. (2021), "Coupled particle swarm optimization method with genetic algorithm for the static–dynamic performance of the magneto-electro-elastic nanosystem", *Eng. Comput.*, 1-15. https://doi.org/10.1007/s00366-021-01391-x.

Kumar, Y., Gupta, A. and Tounsi, A. (2021), "Size-dependent vibration response of porous graded nanostructure with FEM and nonlocal continuum model", *Adv. Nano Res.*, **11**(1), 1-17. https://doi.org/10.12989/anr.2021.11.1.001.

Lee, W.Y., Stinton, D.P., Berndt, C.C., Erdogan, F., Lee, Y.D. and Mutasim, Z. (1996), "Concept of functionally graded materials for advanced thermal barrier coating applications", *J. Am. Ceram. Soc.*, **79**(12), 3003-3012. https://doi.org/10.1111/j.1151-2916.1996.tb08070.x.

Lestari, W. and Hanagud, S. (2001), "Nonlinear vibration of buckled beams: some exact solutions", *Int. J. Solid Struct.*, **38**(26-27), 4741-4757. https://doi.org/10.1016/S0020-7683(00)00300-0.

Li, J., Tang, F. and Habibi, M. (2020a), "Bi-directional thermal buckling and resonance frequency characteristics of a GNP-reinforced composite nanostructure", *Eng. Comput.*, 1-22. https://doi.org/10.1007/s00366-020-01110-y.

Li, Y., Li, S., Guo, K., Fang, X. and Habibi, M. (2020b), "On the modeling of bending responses of graphene-reinforced higher order annular plate via two-dimensional continuum mechanics approach", *Eng. Comput.*, 1-22. https://doi.org/10.1007/s00366-020-01166-w.

Li, X., Yang, H., Zhang, J., Qian, G., Yu, H. and Cai, J. (2021), "Time-domain analysis of tamper displacement during dynamic compaction based on automatic control", *Coatings*, **11**(9), 1092. https://doi.org/10.3390/coatings11091092.

Lim, C.W., Zhang, G. and Reddy, J.N. (2015), "A higher-order nonlocal elasticity and strain gradient theory and its applications in wave propagation", *J. Mech. Phys. Solids*, **78**, 298-313. https://doi.org/10.1016/j.jmps.2015.02.001.

Liu, Z., Meyers, M.A., Zhang, Z. and Ritchie, R.O. (2017), "Functional gradients and heterogeneities in biological materials: Design principles, functions, and bioinspired applications", *Prog. Mater. Sci*., **88**, 467-498. https://doi.org/10.1016/j.pmatsci.2017.04.013.

Liu, C., Deng, F., Heng, Q., Cai, X., Zhu, R. and Liserre, M. (2021a), "Crossing thyristor branches-based hybrid modular multilevel converters for DC line faults", *IEEE T. Ind. Electron*., **68**(10), 9719-9730. https://doi.org/10.1109/TIE.2020.3026277.

Liu, C., Gao, X., Chi, D., He, Y., Liang, M. and Wang, H. (2021b), "On-line chatter detection in milling using fast kurtogram and frequency band power", *Eur. J. Mech. A Solids*, **90**, 104341. https://doi.org/10.1016/j.euromechsol.2021.104341.

Liu, Y., Wang, W., He, T., Moradi, Z. and Larco Benítez, M.A. (2021c), "On the modelling of the vibration behaviors via discrete singular convolution method for a high-order sector annular system", *Eng. Comput*., 1-23. https://doi.org/10.1007/s00366-021-01454-z.

Lu, L., Guo, X. and Zhao, J. (2017), "Size-dependent vibration analysis of nanobeams based on the nonlocal strain gradient theory", *Int. J. Eng. Sci*., **116**, 12-24. https://doi.org/10.1016/j.ijengsci.2017.03.006.

Lu, Z.Q., Zhao, L., Ding, H. and Chen, L.Q. (2021), "A dual-functional metamaterial for integrated vibration isolation and energy harvesting", *J. Sound Vib*., **509**, 116251. https://doi.org/10.1016/j.jsv.2021.116251.

Ma, L., Liu, X. and Moradi, Z. (2021), "On the chaotic behavior of graphene-reinforced annular systems under harmonic excitation", *Eng. Comput*., 1-25. https://doi.org/10.1007/s00366-020-01210-9.

Malekzadeh, P. and Shojaee, M. (2013), "Surface and nonlocal effects on the nonlinear free vibration of non-uniform nanobeams", *Compos. Part B Eng*. **52**, 84-92. https://doi.org/10.1016/j.compositesb.2013.03.046.

Matouk, H., Bousahla, A.A., Heireche, H., Bourada, F., Bedia, E., Tounsi, A., Mahmoud, S., Tounsi, A. and Benrahou, K. (2020), "Investigation on hygro-thermal vibration of P-FG and symmetric S-FG nanobeam using integral Timoshenko beam theory", *Adv. Nano Res*., **8**(4), 293-305. https://doi.org/10.12989/anr.2020.8.4.293.

Mindlin, R.D. (1965), "Second gradient of strain and surface-tension in linear elasticity", *Int. J. Solid Struct*., **1**(4), 417-438. https://doi.org/10.1016/0020-7683(65)90006-5.

Mirjavadi Seyed, S., Afshari Behzad, M., Shafiei, N., Hamouda, A.M.S. and Kazemi, M. (2017a), "Thermal vibration of two-dimensional functionally graded (2D-FG) porous Timoshenko nanobeams", *Steel Compos. Struct*., **25**(4), 415-426. https://doi.org/10.12989/SCS.2017.25.4.415.

Mirjavadi, S.S., Afshari, B.M., Shafiei, N., Hamouda, A. and Kazemi, M. (2017b), "Thermal vibration of two-dimensional functionally graded (2D-FG) porous Timoshenko nanobeams", *Steel Compos. Struct*. **25**(4), 415-426. https://doi.org/10.12989/scs.2017.25.4.415.

Mirjavadi, S.S., Matin, A., Shafiei, N., Rabby, S. and Mohasel Afshari, B. (2017c), "Thermal buckling behavior of two-dimensional imperfect functionally graded microscale-tapered porous beam", *J. Therm. Stress.*, **40**(10), 1201-1214. https://doi.org/10.1080/01495739.2017.1332962.

Mirjavadi, S.S., Mohasel Afshari, B., Shafiei, N., Rabby, S. and Kazemi, M. (2017d), "Effect of temperature and porosity on the vibration behavior of two-dimensional functionally graded micro-scale Timoshenko beam", *J. Vib. Control.*, **24**(18), 4211-4225. https://doi.org/10.1177/1077546317721871.

Mirjavadi, S.S., Rabby, S., Shafiei, N., Afshari, B.M. and Kazemi, M. (2017e), "On size-dependent free vibration and thermal buckling of axially functionally graded nanobeams in thermal environment", *Appl. Phys. A*, **123**(5), 315. https://doi.org/10.1007/s00339-017-0918-1.

Mirzaei, M. and Kiani, Y. (2016), "Nonlinear free vibration of temperature-dependent sandwich beams with carbon nanotube-reinforced face sheets", *Acta Mechanica*, **227**(7), 1869-1884. https://doi.org/10.1007/s00707-016-1593-6.

Mohammadi, M., Hosseini, M., Shishesaz, M., Hadi, A. and Rastgoo, A. (2019), "Primary and secondary resonance analysis of porous functionally graded nanobeam resting on a nonlinear foundation subjected to mechanical and electrical loads", *Eur. J. Mech. A Solid*, **77**, 103793. https://doi.org/10.1016/j.euromechsol.2019.05.008.

Moradi, Z., Davoudi, M., Ebrahimi, F. and Ehyaei, A.F. (2021), "Intelligent wave dispersion control of an inhomogeneous micro-shell using a proportional-derivative smart controller", *Wave Random Complex*, 1-24, https://doi.org/10.1080/17455030.2021.1926572.

Mueller, E., Drašar, Č., Schilz, J. and Kaysser, W. (2003), "Functionally graded materials for sensor and energy applications", *Mater. Sci. Eng. A*, **362**(1-2), 17-39. https://doi.org/10.1016/S0921-5093(03)00581-1.

Navi, B.R., Mohammadimehr, M. and Arani, A.G. (2019), "Active control of three-phase CNT/resin/fiber piezoelectric polymeric nanocomposite porous sandwich microbeam based on sinusoidal shear deformation theory", *Steel Compos. Struct*., **32**(6), 753-767. https://doi.org/10.12989/scs.2019.32.6.753.

Ni, T., Liu, D., Xu, Q., Huang, Z., Liang, H. and Yan, A. (2020), "Architecture of Cobweb-Based Redundant TSV for Clustered Faults", *IEEE T. VLSI Syst*., **28**(7), 1736-1739 https://doi.org/10.1109/TVLSI.2020.2995094.

Ni, T., Yang, Z., Chang, H., Zhang, X., Lu, L., Yan, A., Huang, Z. and Wen, X. (2021), "A novel TDMA-based fault tolerance technique for the TSVs in 3D-ICs using honeycomb topology", *IEEE T. Emerg. Topic Comput*., **9**(2), 724-734 https://doi.org/10.1109/TETC.2020.2969237.

Pompe, W., Worch, H., Epple, M., Friess, W., Gelinsky, M., Greil, P., Hempel, U., Scharnweber, D. and Schulte, K. (2003), "Functionally graded materials for biomedical applications", *Mater. Sci. Eng. A*, **362**(1-2), 40-60. https://doi.org/10.1016/S0921-5093(03)00580-X.

Reddy, J.N. and Chin, C.D. (1998), "Thermomechanical analysis of functionally graded cylinders and plates", *J. Therm. Stress*, **21**(6), 593-626. https://doi.org/10.1080/01495739808956165.

Reddy, J.N. (2007), "Nonlocal theories for bending, buckling and vibration of beams", *Int. J. Eng. Sci*.,. **45**(2), 288-307. https://doi.org/10.1016/j.ijengsci.2007.04.004.

Shafiei, N., Kazemi, M. and Ghadiri, M. (2016a), "Comparison of modeling of the rotating tapered axially functionally graded Timoshenko and Euler–Bernoulli microbeams", *Physica E*, **83**, 74-87. https://doi.org/10.1016/j.physe.2016.04.011.

Shafiei, N., Kazemi, M. and Ghadiri, M. (2016b), "Nonlinear vibration behavior of a rotating nanobeam under thermal stress using Eringen's nonlocal elasticity and DQM", *Appl. Phys. A*, **122**(8), 728. https://doi.org/10.1007/s00339-016-0245-y.

Shafiei, N., Kazemi, M. and Ghadiri, M. (2016c), "Nonlinear vibration of axially functionally graded tapered microbeams", *Int. J. Eng. Sci*.,. **102**, 12-26. https://doi.org/10.1016/j.ijengsci.2016.02.007.

Shafiei, N., Kazemi, M. and Ghadiri, M. (2016d), "On size-

dependent vibration of rotary axially functionally graded microbeam", *Int. J. Eng. Sci*., **101**, 29-44. https://doi.org/10.1016/j.ijengsci.2015.12.008.

Shafiei, N., Kazemi, M., Safi, M. and Ghadiri, M. (2016e), "Nonlinear vibration of axially functionally graded non-uniform nanobeams", *Int. J. Eng. Sci*.,. **106**, 77-94. https://doi.org/10.1016/j.ijengsci.2016.05.009.

Shafiei, N., Mousavi, A. and Ghadiri, M. (2016f), "On size-dependent nonlinear vibration of porous and imperfect functionally graded tapered microbeams", *Int. J. Eng. Sci*., **106**, 42-56. https://doi.org/10.1016/j.ijengsci.2016.05.007.

Shafiei, N., Mousavi, A. and Ghadiri, M. (2016g), "Vibration behavior of a rotating non-uniform FG microbeam based on the modified couple stress theory and GDQEM", *Compos. Struct*., **149**, 157-169. https://doi.org/10.1016/j.compstruct.2016.04.024.

Shafiei, N. and Kazemi, M. (2017a), "Buckling analysis on the bi-dimensional functionally graded porous tapered nano-/micro-scale beams", *Aerosp. Sci. Technol*., **66**, 1-11. https://doi.org/10.1016/j.ast.2017.02.019.

Shafiei, N. and Kazemi, M. (2017b), "Nonlinear buckling of functionally graded nano-/micro-scaled porous beams", *Compos. Struct*., **178** 483-492. https://doi.org/10.1016/j.compstruct.2017.07.045.

Shafiei, N., Ghadiri, M., Makvandi, H. and Hosseini, S.A. (2017a), "Vibration analysis of Nano-Rotor's Blade applying Eringen nonlocal elasticity and generalized differential quadrature method", *Appl. Math. Model*., **43**, 191-206. https://doi.org/10.1016/j.apm.2016.10.061.

Shafiei, N., Kazemi, M. and Fatahi, L. (2017b), "Transverse vibration of rotary tapered microbeam based on modified couple stress theory and generalized differential quadrature element method", *Mech. Adv. Mater. Struct*., **24**(3), 240-252, https://doi.org/10.1080/15376494.2015.1128025.

Shafiei, N., Mirjavadi, S.S., Afshari, B.M., Rabby, S. and Hamouda, A.M.S. (2017c), "Nonlinear thermal buckling of axially functionally graded micro and nanobeams", *Compos. Struct*., **168**, 428-439. https://doi.org/10.1016/j.compstruct.2017.02.048.

Shafiei, N., Mirjavadi, S.S., MohaselAfshari, B., Rabby, S. and Kazemi, M. (2017d), "Vibration of two-dimensional imperfect functionally graded (2D-FG) porous nano-/micro-beams", *Comput. Method Appl. M*., **322**, 615-632. https://doi.org/10.1016/j.cma.2017.05.007.

Shafiei, N. and She, G.L. (2018), "On vibration of functionally graded nano-tubes in the thermal environment", *Int. J. Eng. Sci*., **133**, 84-98. https://doi.org/10.1016/j.ijengsci.2018.08.004.

Shafiei, N., Ghadiri, M. and Mahinzare, M. (2019), "Flapwise bending vibration analysis of rotary tapered functionally graded nanobeam in thermal environment", *Mech. Adv. Mater. Struct*., **26**(2), 139-155. https://doi.org/10.1080/15376494.2017.1365982.

Shafiei, N., Hamisi, M. and Ghadiri, M. (2020), "Vibration analysis of rotary tapered axially functionally graded Timoshenko nanobeam in thermal environment", *J. Solid Mech*., **12**(1), 16-32. https://doi.org/10.22034/jsm.2019.563759.1273.

Shariati, A., Habibi, M., Tounsi, A., Safarpour, H. and Safa, M. (2021), "Application of exact continuum size-dependent theory for stability and frequency analysis of a curved cantilevered microtubule by considering viscoelastic properties", *Eng. Comput*., **37**(4), 3629-3648. https://doi.org/10.1007/s00366-020-01024-9.

Şimşek, M. (2016), "Nonlinear free vibration of a functionally graded nanobeam using nonlocal strain gradient theory and a novel Hamiltonian approach", *Int. J. Eng. Sci*., **105**, 12-27. https://doi.org/10.1016/j.ijengsci.2016.04.013.

Srinivas, P., Babu, P.R. and Balakrishna, B. (2019), "Effect of silicon carbide, magnesium oxide as reinforcing elements and zinc sterate as binding agent in the characterization of Al functionally graded materials for automotive applications", *Mater. Today Proc*., **27**, 460-466. https://doi.org/10.1016/j.matpr.2019.11.275.

Tahir, S.I., Chikh, A., Tounsi, A., Al-Osta, M.A., Al-Dulaijan, S.U. and Al-Zahrani, M.M. (2021a), "Wave propagation analysis of a ceramic-metal functionally graded sandwich plate with different porosity distributions in a hygro-thermal environment", *Compos. Struct*., **269**, 114030. https://doi.org/10.1016/j.compstruct.2021.114030.

Tahir, S.I., Tounsi, A., Chikh, A., Al-Osta, M.A., Al-Dulaijan, S.U. and Al-Zahrani, M.M. (2021b), "An integral four-variable hyperbolic HSDT for the wave propagation investigation of a ceramic-metal FGM plate with various porosity distributions resting on a viscoelastic foundation", *Wave Random Complex*, 1-24, https://doi.org/10.1080/17455030.2021.1942310.

Tong, G., Liu, Y., Cheng, Q. and Dai, J. (2020), "Stability analysis of cantilever functionally graded material nanotube under thermo-magnetic coupling effect", *Eur. J. Mech. A Solid*, **80**, 103929. https://doi.org/10.1016/j.euromechsol.2019.103929.

Wang, M., Li, Z.M. and Qiao, P. (2016), "Semi-analytical solutions to buckling and free vibration analysis of carbon nanotube-reinforced composite thin plates", *Compos. Struct*., **144**, 33-43. https://doi.org/10.1016/j.compstruct.2016.02.025.

Wang, P., Wang, S.Z., Kang, Y.R., Sun, Z.S., Wang, X.D., Meng, Y., Hong, M.H. and Xie, W.F. (2021), "Cauliflower-shaped Bi2O3–ZnO heterojunction with superior sensing performance towards ethanol", *J. Alloy Compd*., **854**, 157152. https://doi.org/10.1016/j.jallcom.2020.157152.

Xu, W., Pan, G., Moradi, Z. and Shafiei, N. (2021), "Nonlinear forced vibration analysis of functionally graded non-uniform cylindrical microbeams applying the semi-analytical solution", *Compos. Struct*., **275**, 114395. https://doi.org/10.1016/j.compstruct.2021.114395.

Yu, X., Maalla, A. and Moradi, Z. (2022), "Electroelastic high-order computational continuum strategy for critical voltage and frequency of piezoelectric NEMS via modified multi-physical couple stress theory", *Mech. Syst. Signal Pr*., **165**, 108373. https://doi.org/10.1016/j.ymssp.2021.108373.

Zhang, L., Lei, Z. and Liew, K. (2015), "Vibration characteristic of moderately thick functionally graded carbon nanotube reinforced composite skew plates", *Compos. Struct*., **122**, 172-183. https://doi.org/10.1016/j.compstruct.2014.11.070.

Zhang, B., Chen, Y.X., Wang, Z.G., Li, J.Q. and Ji, H.H. (2021a), "Influence of mach number of main flow on film cooling characteristics under supersonic condition", **13**(1), 127. https://doi.org/10.3390/sym13010127.

Zhang, L., Wang, X., Zhang, Z., Cui, Y., Ling, L. and Cai, G. (2021b), "An adaptative control strategy for interfacing converter of hybrid microgrid based on improved virtual synchronous generator", *IET Renew. Power Gener*. https://doi.org/10.1049/rpg2.12293.

Zhao, X., Chen, B., Li, Y.H., Zhu, W.D., Nkiegaing, F.J. and Shao, Y.B. (2020), "Forced vibration analysis of Timoshenko double-beam system under compressive axial load by means of Green's functions", *J. Sound Vib*., **464**, 115001. https://doi.org/10.1016/j.jsv.2019.115001.

Zhao, X., Zhu, W.D. and Li, Y.H. (2020), "Analytical solutions of nonlocal coupled thermoelastic forced vibrations of micro-/nano-beams by means of Green's functions", *J. Sound Vib*., **481**, 115407. https://doi.org/10.1016/j.jsv.2020.115407.

Zhao, Y., Moradi, Z., Davoudi, M. and Zhuang, J. (2021), "Bending and stress responses of the hybrid axisymmetric system via state-space method and 3D-elasticity theory", *Eng. Comput*., 1-23. https://doi.org/10.1007/s00366-020-01242-1.

Zhong, Q., Yang, J., Shi, K., Zhong, S., Li, Z. and Sotelo, M.A.

(2021), "Event-triggered H_∞ load frequency control for multi-area nonlinear power systems based on non-fragile proportional integral control strategy", *IEEE T. Intell. Transp.*, 1-11, https://doi.org/10.1109/TITS.2021.3110759.

Zine, A., Bousahla, A.A., Bourada, F., Benrahou, K.H., Tounsi, A., Adda Bedia, E., Mahmoud, S. and Tounsi, A. (2020), "Bending analysis of functionally graded porous plates via a refined shear deformation theory", *Comput. Concrete*, **26**(1), 63-74. https://doi.org/10.12989/cac.2020.26.1.063.